# The Tropopause in the Polar Regions

GÜNTHER ZÄNGL

*Meteorologisches Institut der Universität München, Munich, Germany*

KLAUS P. HOINKA

*Institut für Physik der Atmosphäre, DLR Oberpfaffenhofen, Wesseling, Germany*

(Manuscript received 24 July 2000, in final form 28 November 2000)

ABSTRACT

The polar and subpolar tropopause in both hemispheres is investigated using the ECMWF Reanalysis (ERA) data from 1979 to 1993 and radiosonde data from 1989 to 1993. Both the thermal and the dynamical criteria are applied to each dataset. The tropopauses derived from the radiosonde data are used to validate the ERA-derived tropopauses and to investigate the sharpness of the tropopause. The validation reveals that the ERA data are well suited for the determination of the tropopause. A comparison between the thermal and the dynamical tropopause shows a very good agreement except for polar winter, and there is clear evidence that the dynamical criterion is more appropriate in winter.

The results show that the annual cycle of the polar tropopause can be classified into three different patterns. A single wave with a tropopause pressure maximum in winter and a minimum in summer is typical for the subpolar parts of eastern Siberia and North America. A double wave with pressure maxima in spring and autumn and minima in summer and winter is found above northern Europe, western Siberia, and generally at high Arctic latitudes. Finally, Antarctica exhibits a reversed single wave with a pressure maximum in summer and a minimum in winter. Tropopause temperatures are generally highest in summer and lowest in winter, but the amplitude of their annual cycles shows distinct differences. It is lowest in those regions where a single pressure maximum in winter is present and largest in the Antarctic. A comparison between the tropopause pressure and the temperatures in 500 and 100 hPa reveals that the tropopause pressure is closely related to the temperature difference between 500 and 100 hPa. A large temperature difference corresponds to a low tropopause pressure and a small temperature difference to a high tropopause pressure. The sharpness of the tropopause, that is, the change in vertical temperature gradient across the tropopause, is found to be highest in summer and lowest in winter. Its annual cycle and its regional differences are primarily determined by the mean temperature gradient above the tropopause because it varies much more strongly than the gradient below the tropopause.

## 1. Introduction

The tropopause is one of the basic features of the earth's atmosphere. It separates the troposphere, which is marked by a relatively low static stability, from the stably stratified stratosphere. Besides the stratification, there are several other atmospheric properties in which the stratosphere differs significantly from the troposphere, for example, moisture and the ozone concentration. Hence, it is not surprising that the tropopause has received increasing interest during the last two or three decades. A major part of the literature deals with exchange processes through the tropopause (e.g., Shapiro 1980; Wirth 1995) or attempts to estimate the amount of the mass exchange through the tropopause (e.g., Holton 1990; Ebel et al. 1996). The importance of this mass exchange lies in its impact on atmospheric chemistry. For example, stratospheric ozone chemistry involves many trace constituents whose sources are in the troposphere.

The literature on the tropopause itself concentrates mainly on the tropical tropopause and, especially, on its temperature. Since the upward branch of the Brewer–Dobson circulation is located in the Tropics, the tropical tropopause temperature controls the stratospheric water vapor mixing ratio. However, the mean tropical tropopause temperature is still too high to account for the observed extreme dryness of the stratosphere. According to Newell and Gould-Stewart (1981), Indonesia is the only region where the tropopause is really cold enough. Therefore, they have suggested that most of the tropical upwelling occurs in that region (see also Frederick and Douglass 1983). Another interesting feature of the tropical tropopause is its annual cycle that is related to the annual cycle of the stratospheric meridional circulation (Yulaeva et al. 1994; Reid and Gage

*Corresponding author address:* Dr. Günther Zängl, Meteorologisches Institut der Universität München, Theresienstraße 37, D-80333 München, Germany.
E-mail: guenther@meteo.physik.uni-muenchen.de

1996). A first climatology of the tropical tropopause has been presented by Highwood and Hoskins (1998).

Comparatively little work has been done on the extratropical tropopause. Although Appenzeller et al. (1996) pointed out that a significant amount of stratosphere–troposphere exchange may occur due to the annual cycle of the mean tropopause pressure, there appears to be only one global tropopause climatology (Hoinka 1998, hereafter H98; Hoinka 1999). Moreover, these studies did not focus on the annual cycle of the tropopause. Hoinka considered only seasonal means of summer and winter, which may be too coarse to resolve the annual cycle. In fact, the study of Highwood et al. (2000, hereafter HHB), who investigated the Arctic tropopause in more detail, suggests a double wave with maxima of the tropopause pressure in spring and autumn and minima in summer and winter. However, detailed studies of the tropopause in the remaining extratropical regions are still missing. In particular, the Antarctic tropopause deserves further research because of the difficulties in determining it in winter. As has already been recognized by Court (1942), the tropopause is very indistinct in Antarctic winter so that it is questionable whether the common thermal criterion is applicable in this case. The same question may be posed on the Arctic winter tropopause although HHB state that its determination with the thermal criterion is unproblematic. A detailed investigation of the sharpness of the polar tropopause and a comparison between different tropopause criteria are needed to answer these questions.

The main goal of this paper is to fill these gaps in the knowledge of the polar tropopause. Moreover, the study is extended to the subpolar regions in order to capture the transition between the polar regions and middle latitudes. The data analysis is mainly based on the European Centre for Medium-Range Weather Forecasts (ECMWF) reanalysis (ERA) data for the period 1979–93, which have already been used by H98. Compared with the original ECMWF analysis data, the ERA dataset has the advantage to constitute a homogeneous dataset (see H98 for a more thorough discussion). New algorithms are used to determine both the thermal and the dynamical tropopause from this dataset. They have been validated against a 5-yr set of radiosonde data for both polar regions. In order to extend this validation to the dynamical tropopause, an additional algorithm has been developed for the determination of the dynamical tropopause from the radiosonde data. It uses interpolated vorticity fields from the ERA data because the density of radiosonde stations is too low in the polar regions to compute the vorticity from the radiosonde wind data. Since the thermal tropopause criterion has been found to be inadequate for Antarctic winter, the dynamical criterion is taken as standard in this paper. One section will be devoted to the comparison between the thermal and the dynamical criterion. For tropopause pressure and temperature, the discussion is restricted the ERA-derived fields. However, the radiosonde data are used to evaluate the sharpness of the tropopause because the vertical resolution of the ERA data is too coarse for this purpose.

The outline of this paper is as follows. A brief description of the datasets is given in section 2. Section 3 presents the tropopause criteria and their application to the data. The validation of the new algorithms is described in section 4. In section 5, climatological fields of tropopause pressure and tropopause temperature are presented. The annual cycle of the tropopause pressure is discussed in more detail in section 6. Section 7 gives a comparison between the thermal and the dynamical tropopause and an analysis of the differences between them. The sharpness of the tropopause, that is, the amount of change in the vertical temperature gradient across the tropopause, is considered in section 8. Finally, a summary of the main results is given in section 9. Some details of the new algorithms are presented in appendixes A–C.

## 2. Datasets

In the present study, we use the model-level ERA data on the latitude–longitude grid. Compared to the standard pressure-level data, which are also available from the ECMWF, the model-level data have approximately twice as many levels (31 instead of 15) and, therefore, a better vertical resolution. This is especially valid in the tropopause region, so that the model-level data are certainly more appropriate for the determination of the tropopause. In addition, the smoothing of the meteorological fields inherent in the interpolation from the model levels to the standard pressure levels probably would further deteriorate the quality of the ERA-derived tropopauses. The horizontal resolution of the data is $1.125^\circ \times 1.125^\circ$, corresponding to their spectral resolution of T106.

The radiosonde data used in this study cover the regions poleward of 55°N and 50°S, respectively, and the time period from 1989 to 1993. The locations of the radiosonde stations are displayed in Fig. 1. The data have been provided by the German Weather Service (Deutscher Wetterdienst, DWD). According to the standard World Meteorological Organization (WMO) TEMP format, this dataset includes explicitly reported thermal tropopauses (see below). Since the radiosonde data had not been checked for coding or measurement errors, some simple quality checks were applied. The reported tropopauses were checked for consistency with the sounding, and the soundings were checked for strongly overadiabatic temperature gradients. If overadiabatic gradients could be eliminated by removing a single data point, this point was assumed to be a coding error and was removed. However, if a sounding contained more than two errors, the whole sounding was not taken into account. If the reported tropopause was inconsistent with the WMO criterion, the tropopause was calculated directly from the sounding. Finally, the

500- and 100-hPa temperatures were checked against the respective values interpolated from the ERA data. Since the majority of data points was less than 3 K apart, differences of more than 4 K were taken as an indication that the sounding had been eliminated during the data assimilation cycle at the ECMWF.

The data analysis reported in this paper is restricted to 1200 UTC. A preliminary analysis of the radiosonde data had shown that the diurnal cycle of the tropopause pressure is negligible.

## 3. Tropopause criteria

### *a. Thermal tropopause*

The thermal tropopause definition is based on the fact that the stratosphere is more stably stratified than the troposphere. In terms of the lapse rate, which is defined as the vertical temperature gradient multiplied by $-1$, this means that the stratospheric lapse rate is lower than the tropospheric one. According to WMO (1957), the thermal tropopause is defined as ''the lowest level at which the lapse rate decreases to 2 K km$^{-1}$ or less, provided also the average lapse rate between this level and all higher levels within 2 km does not exceed 2 K km$^{-1}$.'' The determination of the thermal tropopause from the ERA data starts with a calculation of the vertical temperature gradients between the model levels. They are assigned to intermediate levels, corresponding to centered differences. Then, the level that fulfills both parts of the lapse rate criterion is searched, and the exact value of the tropopause height is computed under the assumption that the vertical temperature gradient varies linearly with height in the tropopause region. The tropopause pressure is interpolated between the model levels under the assumption $z \sim \ln p$, where $z$ and $p$ are height and pressure, respectively. Finally, the tropopause temperature is determined by extrapolating the temperature gradient above or below the tropopause. A detailed description of this algorithm is given in appendix A. It is noted that taking into account the second part of the WMO criterion (henceforth referred to as thickness criterion) is definitely necessary. A comparison with radiosonde-derived tropopauses (see section 4) revealed that the quality of the ERA-derived tropopauses is deteriorated substantially if the thickness criterion is neglected. Moreover, it will be shown in section 4 that the extrapolation of the tropopause temperature yields significantly better results than the common interpolation, which induces a warm bias (see also Highwood and Hoskins 1998).

### *b. Dynamical tropopause*

An alternative to the thermal criterion, based on potential vorticity (PV), was first proposed by Reed (1955). The hydrostatic form of the PV in height coordinates is given by

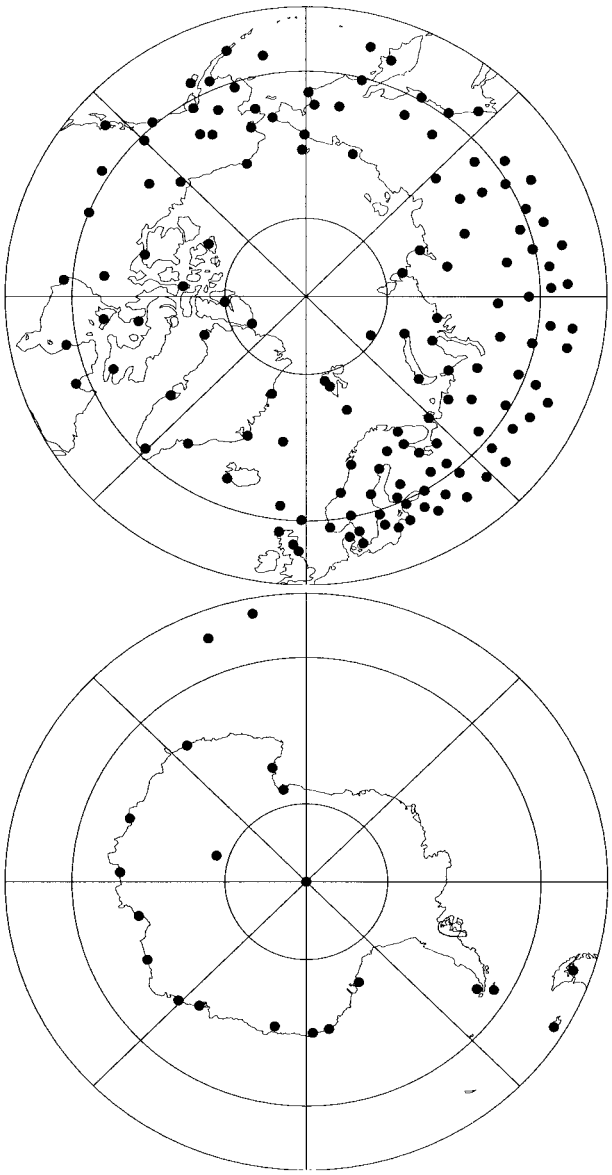

FIG. 1. Locations of the radiosonde stations poleward of (top) 55°N and (bottom) 50°S. Latitude circles are shown for 80° and 60°.

$$P = \frac{1}{\rho}(f\mathbf{k} + \boldsymbol{\nabla} \times \mathbf{v}) \cdot \boldsymbol{\nabla}\theta, \tag{1}$$

where $\rho$ is the density, $f$ is the Coriolis parameter, $\mathbf{k}$ is the unit vector in the vertical, $\mathbf{v} = (u, v)$ is the horizontal wind vector, and $\theta$ is the potential temperature. In contrast to the vertical temperature gradient, $P$ is materially conserved for adiabatic motions. Therefore, it can be argued that $P$ is more appropriate to divide stratospheric air from tropospheric air than $\partial T/\partial z$, especially in cyclogenetically active regions.

From Eq. (1), it is clear that the stratosphere is marked by higher absolute PV values than the troposphere, the sign of the PV being positive in the Northern Hemi-

sphere (NH) and negative in the Southern Hemisphere (SH). In the following, only the NH case is considered. Using the PV unit (PVU), which is defined as 1 PVU $= 10^{-6}$ K m$^2$ kg$^{-1}$ s$^{-1}$, tropospheric air can be characterized by PV values of $\lesssim$1 PVU, while stratospheric air typically has $P \gtrsim 5$ PVU. Thus, the PV threshold used as tropopause definition must be somewhere in between these values. However, there is still no generally accepted value. The WMO (1986) suggested a threshold of 1.6 PVU, but most authors use values between 2 and 3.5 PVU. A comparison between the thermal tropopause and the dynamical tropopause with threshold values ranging between 1 and 5 PVU was performed by Hoerling et al. (1991). They found that the pressure of the dynamical tropopause is systematically higher than that of the thermal tropopause for values less than 3 PVU while it is systematically lower for values greater than 4 PVU. The best agreement was found for a threshold value of 3.5 PVU. Therefore, Hoerling et al. suggested this value to delineate the dynamical tropopause.

One may argue against this method of determining an ''optimal'' threshold for the PV tropopause that the thermal criterion is itself—at least to a certain extent—arbitrary and, therefore, not a suitable reference. Moreover, the thermal criterion is not able to characterize air masses because the vertical temperature gradient is not a conserved quantity. There are, however, other arguments to use a higher value than 1.6 PVU, especially in the polar regions. First, our data analysis revealed that the 1.6 PVU surface frequently descends below the 700-hPa level in polar winter. Under very strong cyclonic influence, it is even possible that the 1.6 PVU surface intersects the ground. Second, the comparison between radiosonde-derived tropopauses and ERA-derived tropopauses (see next section) showed that the correlation between them is much worse for 1.6 PVU than for 3.5 PVU, indicating that a threshold of 1.6 PVU does not yield well-defined, reproducible results. Third, there are too many cases where the 1.6 PVU criterion, applied to the radiosonde data, detects multiple tropopauses. Certainly, some of them can be interpreted as tropopause folds, but the percentage of multiple tropopauses (up to 70% in winter) is more than an order of magnitude larger than the percentage of tropopause folds found in previous studies (e.g., van Haver et al. 1996). All this suggests that 1.6 PVU is not an appropriate tropopause criterion at least at higher latitudes. A higher value or a latitude-dependent value that is higher at polar latitudes is needed to separate stratospheric air from tropospheric air.

Following Hoerling et al. (1991) and H98, a constant value of 3.5 PVU is used in this paper to define the dynamical tropopause. According to Grewe and Dameris (1996), a constant threshold value is more appropriate than a latitude-dependent value if the attention is restricted to polar latitudes. The algorithm to determine the PV tropopause from the ERA data is quite similar to that used for the thermal tropopause. First, the PV according to Eq. (1) is calculated between each two adjacent model levels and assigned to intermediate levels. Then, the level where the threshold value is met is determined, and the tropopause height is calculated under the assumption that the PV varies linearly with height in the tropopause region. Tropopause pressure and temperature are determined as for the thermal tropopause. The detailed description of this algorithm and the algorithm for the calculation of the dynamical tropopause from the radiosonde data are given in appendixes B and C, respectively. In addition, an empirical correction of the ERA-derived pressure of the dynamical tropopause is described that has been used to minimize systematical errors (appendix B).

It should be noted that a thickness criterion similar to the second part of the thermal WMO criterion has been introduced into the PV criterion. It requires that the mean potential vorticity between the tropopause and all levels within 2 km above the tropopause remains above 3.5 PVU. A thickness criterion like this has proved to be very important when calculating the dynamical tropopause from radiosonde data because thin layers of enhanced stability (e.g., subsidence inversions) may otherwise be misinterpreted as the tropopause. However, it may be omitted when using the ERA data except in Antarctic winter, which means that it is not as important as in the thermal tropopause case. Nevertheless, we suggest to incorporate some kind of thickness criterion into the definition of the dynamical tropopause so as to reduce the sensitivity to the vertical resolution of the data. Otherwise, higher-resolution datasets, which will presumably become available during the next years, may not yield reproducible dynamical tropopauses.

## 4. Validation of the ERA-derived tropopauses

For the last five years of the ECMWF reanalysis period, that is, 1989–93, all available radiosonde data poleward of 55°N and 50°S, respectively, (see Fig. 1) have been evaluated in order to validate the tropopauses derived from the ERA data. To compare the different datasets, the ERA tropopause fields are first interpolated linearly to the locations of the radiosonde stations. Then, the data are averaged over months and certain geographical areas. In the Northern Hemisphere, two latitude belts (55°–65°N, 65°–90°N) and four longitude sectors (45°W–45°E, 45°–135°E, 135°E–135°W, 135°–45°W) are distinguished. The longitude sectors are chosen such that regions with similar tropopause properties are put together (cf. Figs. 3–6). In the SH, the sparse density of radiosonde stations allows only for a subdivision into two regions, namely 50°–55°S and 62°–90°S (Antarctica).[1] The number of data points per month

[1] There are no radiosonde stations between 55° and 62°S.

TABLE 1. Annual mean statistics for differences between ERA-derived and radiosonde-derived tropopauses (1989–93; 1200 UTC). Pressure differences and differences of the standard deviation are given in hPa; values in brackets are rms differences.

| | Thermal tropopause | | Dynamical tropopause | | |
|---|---|---|---|---|---|
| Region | Pressure difference | Correlation coefficient | Pressure difference | Std dev difference | Correlation coefficient |
| 55°–65°N, 45°W–45°E | 3.2 (3.3) | 0.923 | −1.7 (1.7) | −3.2 | 0.953 |
| 55°–65°N, 45°–135°E | 1.1 (2.1) | 0.911 | −2.1 (2.4) | −3.4 | 0.947 |
| 55°–65°N, 135°E–135°W | 3.6 (4.0) | 0.893 | −0.8 (1.6) | −2.9 | 0.935 |
| 55°–65°N, 135°–45°W | 2.9 (3.6) | 0.904 | −2.0 (2.4) | −2.7 | 0.941 |
| 65°–90°N, 45°W–45°E | 4.3 (4.8) | 0.908 | −0.5 (1.4) | −2.7 | 0.944 |
| 65°–90°N, 45°–135°E | 0.5 (2.4) | 0.898 | −2.3 (2.7) | −2.9 | 0.938 |
| 65°–90°N, 135°E–135°W | 2.4 (4.0) | 0.896 | −1.8 (2.8) | −3.1 | 0.929 |
| 65°–90°N, 135°–45°W | 2.8 (4.2) | 0.899 | −1.8 (3.0) | −3.0 | 0.935 |
| 50°–55°S | 5.0 (5.5) | 0.882 | 1.8 (2.9) | 0.0 | 0.934 |
| 62°–90°S | 4.9 (8.3) | 0.775 | 2.9 (4.4) | −0.5 | 0.899 |

and region typically ranges between 1000 and 3500 in the NH regions and between 900 and 1200 in Antarctica. The lowest numbers (∼500) are found at 50°–55°S where there are only four radiosonde stations.

For each of these regions, the monthly mean tropopause pressure, its standard deviation, and the correlation coefficient between ERA- and radiosonde-derived tropopause pressures are computed. The two latter quantities are considered in order to show that the skill of the ERA-derived tropopauses is not restricted to monthly means. Annual mean statistics for these quantities are summarized in Table 1. Moreover, monthly mean tropopause temperatures are compared. Since the differences between the ERA-derived tropopauses and the radiosonde-derived tropopauses are quite similar in most of the regions defined above (see Table 1), only three regions will be discussed in detail. These are 45°W–45°E, >65°N (northern Atlantic and Europe), 55°–65°N, 135°E–135°W (eastern Siberia and Alaska) and <62°S (Antarctica). This selection is sufficient to resolve meridional differences in the Arctic as well as interhemispheric differences.

### *a. Tropopause pressure, monthly means*

First, monthly mean tropopause pressures are compared. ERA–radiosonde differences for the selected regions are shown in Fig. 2a, where thin lines refer to the thermal tropopause and bold lines to the PV tropopause. Annual mean differences for all regions are given in Table 1. In addition, the table shows annual rms values of the ERA–radiosonde differences.

Thermal tropopauses generally show weak differences in winter except for Antarctica where negative differences up to 6 hPa occur. In summer, however, ERA-derived tropopause pressures are systematically too high. The largest differences are again found over Antarctica, reaching up to 15 hPa in March, but substantial differences (5–9 hPa) are also present in the Northern Hemisphere. Comparing all available regions, one finds that differences tend to be slightly larger poleward of 65°N than in subpolar regions. In the annual mean, ERA–radiosonde differences range between 1 and 5 hPa, the largest values being found in the Southern Hemisphere. Annual rms values are somewhat larger because positive and negative deviations are partly compensating for. This is most conspicuous in Antarctica where the mean difference amounts to 5 hPa while the rms difference exceeds 8 hPa.

Systematical differences found for the PV tropopauses are clearly lower in magnitude. Except for Antarctic summer and autumn, they are below 5 hPa, and in several Northern Hemisphere regions, they do not exceed 3 hPa. As evident from Table 1, there is a slight tendency for too low tropopause pressures throughout the north polar region. This primarily arises from negative differences in winter (Fig. 2a), while the differences are close to zero in summer. Since typical regional differences of the tropopause pressure and typical amplitudes of its annual cycle are of order 10–50 hPa (see Figs. 3, 5), it follows that the uncertainties in the determination of the tropopause pressure from the ERA data do not affect the results presented in this paper.

### *b. Tropopause pressure, standard deviation*

The standard deviation of the tropopause pressure can be taken as a measure for the synoptic-scale variability of the tropopause. In the present analysis, it is computed according to

$$\sigma_{p_{\mathrm{TP}}} = \sqrt{\frac{1}{N-1}\sum_{i=1}^{N}(p_{\mathrm{TP}_i} - \overline{p}_{\mathrm{TP}})^2}.$$

The summation extends over all data points (radiosonde stations or interpolated ERA values) of one region, one month, and the period 1989–93. Typical values of $\sigma_{p_{\mathrm{TP}}}$ (dynamical tropopause) are 30–40 hPa in Arctic summer, 40–50 hPa in Arctic winter, 25–35 hPa in Antarctic summer, and 30–40 hPa in Antarctic winter. In the storm track regions, $\sigma_{p_{\mathrm{TP}}}$ reaches 55–65 hPa in winter and spring (cf. H98). The thermal tropopause generally exhibits 3–6 hPa lower $\sigma_{p_{\mathrm{TP}}}$ values than the dynamical

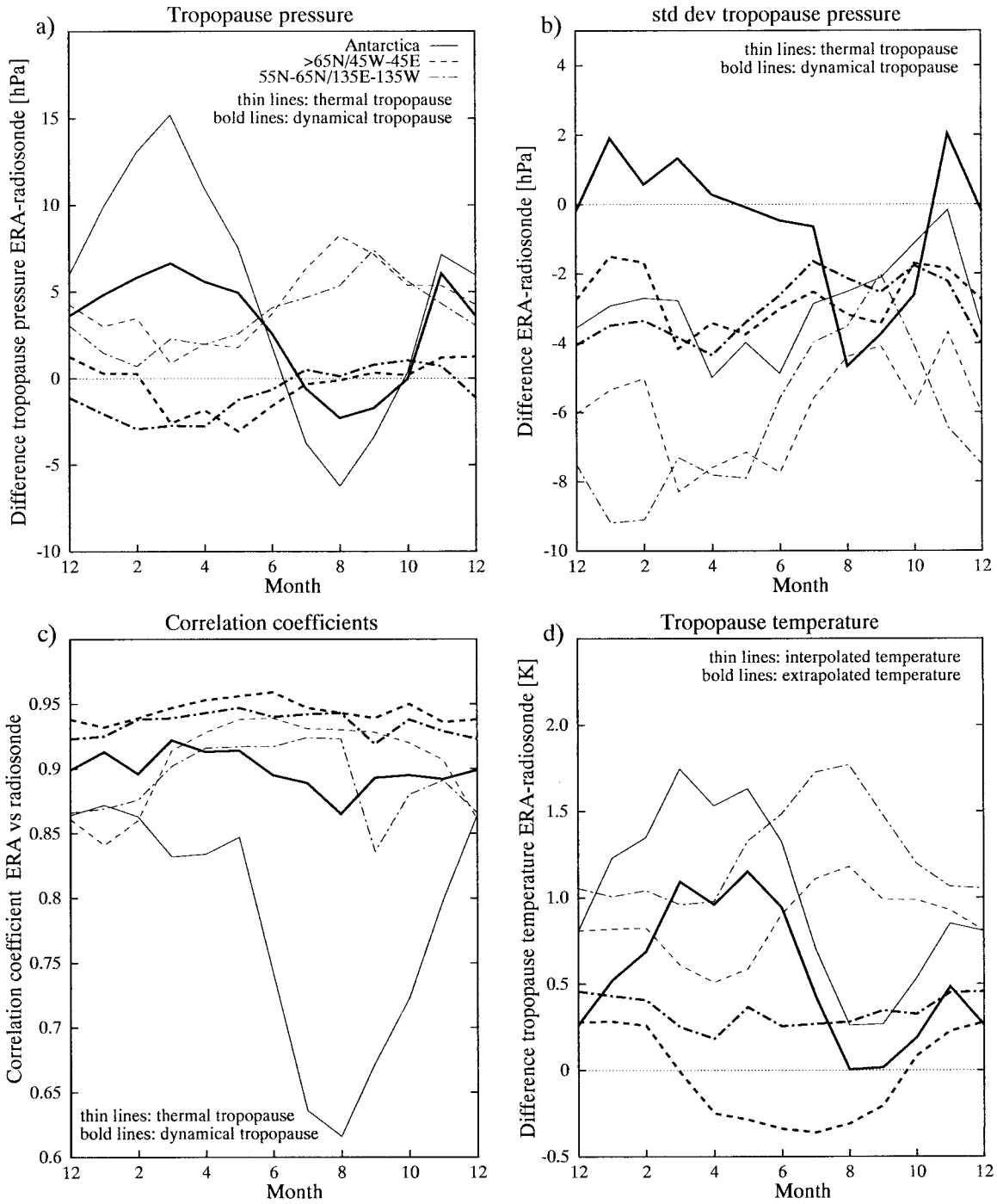


FIG. 2. Differences between ERA-derived tropopauses and radiosonde-derived tropopauses (1989–93; 1200 UTC data): (a) monthly mean tropopause pressure (hPa), (b) standard deviation of the tropopause pressure (hPa), (c) correlation coefficient between ERA-derived and radiosonde-derived tropopause pressure, (d) temperature of the dynamical tropopause (K). In (a)–(c), thin (bold) lines denote the thermal (dynamical) tropopause; in (d), thin (bold) lines denote the interpolated (extrapolated) tropopause temperature.

tropopause except for Antarctic winter where thermal $\sigma_{p_{TP}}$ is about 5 hPa larger.

Comparing $\sigma_{p_{TP}}$ obtained from radiosonde and ERA data (Fig. 2b), one finds that the synoptic-scale variability of the tropopause is slightly underestimated in the ERA data. This underestimation is more pronounced for the thermal tropopause (thin lines) than for the dynamical tropopauses (bold lines). In the Arctic regions, $\sigma^{\mathrm{ERA}}_{p_{TP}} - \sigma^{\mathrm{raso}}_{p_{TP}}$-differences found for the thermal tropopause range between $-4$ hPa in summer and $-9$ hPa

in winter. In the Antarctic, the summer difference is again −4 hPa, but it is close to zero in winter. However, the good coincidence in winter must be considered as fortuitous because of the low correlation between ERA and radiosonde tropopauses (see below). Table 1 shows that the underestimation of $\sigma_{p_{\mathrm{TP}}}$ for the dynamical tropopause is very similar in all parts of the north polar region. In the Southern Hemisphere, there appears to be no systematical underestimation at all, but this result should be taken with care due to the extreme sparsity of data. Nevertheless, we can conclude that the dependence of $\sigma_{p_{\mathrm{TP}}}$ on the dataset in insignificant compared to observed values. This is particularly valid for dynamical tropopauses.

### c. Tropopause pressure, correlation coefficients

To assess the degree of coincidence between radiosonde-derived tropopauses and ERA-derived tropopauses, the correlation coefficient

$$r_{\mathrm{TP}} := \frac{\sum (p_{\mathrm{TP}_i}^{\mathrm{ERA}} - \overline{p_{\mathrm{TP}}^{\mathrm{ERA}}})(p_{\mathrm{TP}_i}^{\mathrm{raso}} - \overline{p_{\mathrm{TP}}^{\mathrm{raso}}})}{\sqrt{\sum (p_{\mathrm{TP}_i}^{\mathrm{ERA}} - \overline{p_{\mathrm{TP}}^{\mathrm{ERA}}})^2 \sum (p_{\mathrm{TP}_i}^{\mathrm{raso}} - \overline{p_{\mathrm{TP}}^{\mathrm{raso}}})^2}}$$

is computed. Summation is again over one region, one month, and the 5-yr period 1989–93. Some examples are given in Fig. 2c, and annual mean values are again summarized in Table 1. In general, it can be stated that PV tropopauses (bold lines) show better correlations than thermal tropopauses (thin lines), especially in winter.

The thermal tropopauses show correlation coefficients between 0.90 and 0.93 in Arctic summer and between 0.81 and 0.89 in Arctic winter, the lowest values occurring in the region >65°N/45°–135°E (not shown). In the Antarctic, $r_{\mathrm{TP}}$ varies between 0.87 in summer and 0.62 in winter. In the annual mean, $r_{\mathrm{TP}}$ ranges between 0.89 and 0.92 in the Northern Hemisphere while a value of only 0.78 is found for Antarctica. The annual cycle of $r_{\mathrm{TP}}$ can be partly explained by the annual cycle of tropopause sharpness (see sections 7 and 8). Due to the low tropopause sharpness typical for winter, little differences between ERA and radiosonde temperature profiles may induce large differences in the tropopause pressure diagnosed by the thermal criterion. This is especially true in Antarctic winter where there are many cases without a well-defined thermal tropopause (section 7).

The $r_{\mathrm{TP}}$ values found for the PV tropopause vary between 0.91 and 0.94 in Arctic winter and between 0.94 and 0.96 in Arctic summer. In the Antarctic, $r_{\mathrm{TP}}$ ranges between 0.86 in winter and 0.92 in summer. The annual mean values are near 0.9 in Antarctica and between 0.93 and 0.95 in the remaining regions. Especially in winter, these values are appreciably better than those obtained for the thermal tropopause. A simple explanation for this can be found in the fact that PV tropopauses are by definition sharper than thermal tropopauses. In an atmosphere with a constant vertical temperature gradient, the PV increases with height proportional to $p^{-(1+\kappa)}$ [see Eq. (C1)]. Therefore, the uncertainty in determining the tropopause induced by a given uncertainty in the data is far lower for the PV definition than for the thermal definition. In some sense, the PV definition may be regarded as numerically more stable than the thermal one. It should be noted that the use of the ERA vorticity data for the calculation of $p_{\mathrm{TP}}^{\mathrm{raso}}$ (see appendix C) cannot be made responsible for the high $r_{\mathrm{TP}}$ values obtained here. Although the relative vorticity is a very important factor, the radiosonde-derived PV tropopauses turned out to coincide with a significant level (i.e., with a change in the vertical temperature gradient) in most cases. Therefore, they would not depend very sensitively on the vorticity data used for their computation.

### d. Tropopause temperature, monthly means

Finally, the tropopause temperatures obtained from the ERA data are discussed. The discussion is restricted to the PV tropopauses because we want to exclude as far as possible tropopause temperature errors resulting from tropopause pressure errors. As shown in Fig. 2d, tropopause temperatures computed by interpolating linearly in $z$ between the neighboring ERA levels exhibit a significant warm bias. They are 1–1.5 K too warm in summer and 0.5–1 K too warm in winter except for Antarctic winter where the bias is below 0.5 K. However, if tropopause temperatures are extrapolated according to (A3), they differ less than 0.5 K from the radiosonde-derived values except for Antarctic summer and autumn. The remaining warm bias over Antarctica can be explained with the positive tropopause pressure bias occurring there (see Fig. 2a). A pressure difference of 6 hPa corresponds to a height difference of about 130 m for $p = 300$ hPa and $T = 225$ K. Assuming $\partial T/\partial z = -6.5$ K km$^{-1}$, this in turn corresponds to a temperature difference of 0.85 K, a value close to the observed warm bias. We conclude that extrapolating the tropopause temperature according to (A3) is clearly superior to the common interpolation method.

Finally, we would like to point out that the temperature bias found by HHB (+2K − +4K) is still substantially larger than that obtained in the present study with the interpolation method. A possible explanation for this may be that HHB did not use intermediate levels for computing vertical temperature gradients (see appendixes A and B).

## 5. Tropopause pressure and temperature

In this section, climatological fields of tropopause pressure and temperature in the polar regions are presented by means of polar stereographic charts. All fields are monthly means and refer to the dynamical tropopause (3.5 PVU) and the period 1979–93. Unlike H98

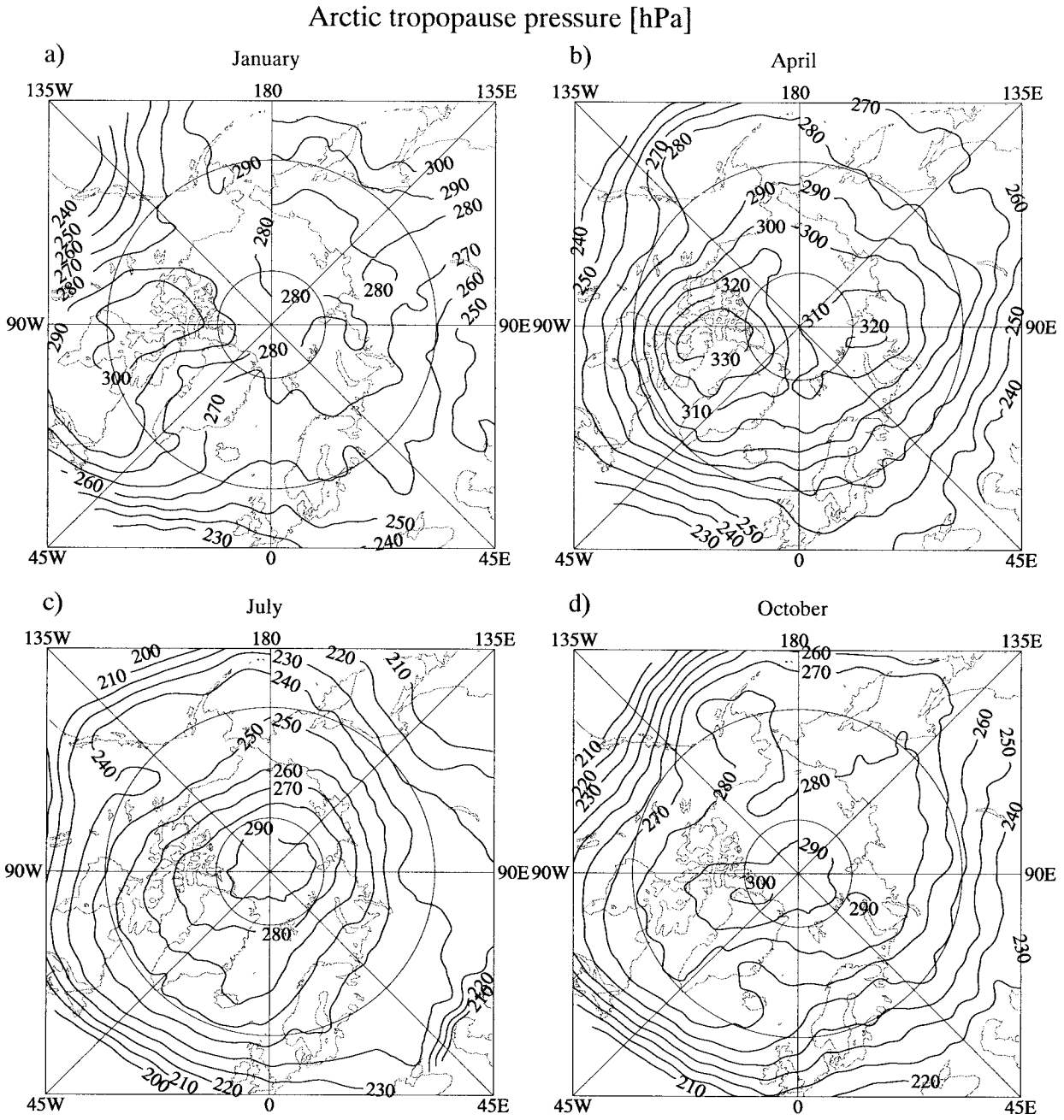


FIG. 3. Polar-stereographic charts of Arctic tropopause pressure (1979–93; 1200 UTC data) for (a) Jan, (b) Apr, (c) Jul, and (d) Oct. Contour interval is 10 hPa. Latitude circles are given for 80° and 60°N; data are shown poleward of 45°N only.

and HHB, who showed seasonal means, we decided to present monthly means in order to avoid excessive smoothing. It will turn out that this is particularly necessary to capture the tropopause temperature minimum in Arctic winter. In order to resolve the annual cycle as well as possible (see below), four months are shown for each hemisphere. These are January, April, July (NH)/August (SH), and October. The August is chosen instead of July in the Antarctic because the extreme values of tropopause pressure and temperature are reached in August there (see section 6). The annual means of the tropopause pressure for both polar regions have already been shown in H98.

### *a. Arctic tropopause*

First, the north polar region is discussed. Tropopause pressure and temperature are shown in Figs. 3 and 4, respectively. In January, the highest tropopause pressure is found over Canada, reaching slightly above 300 hPa.

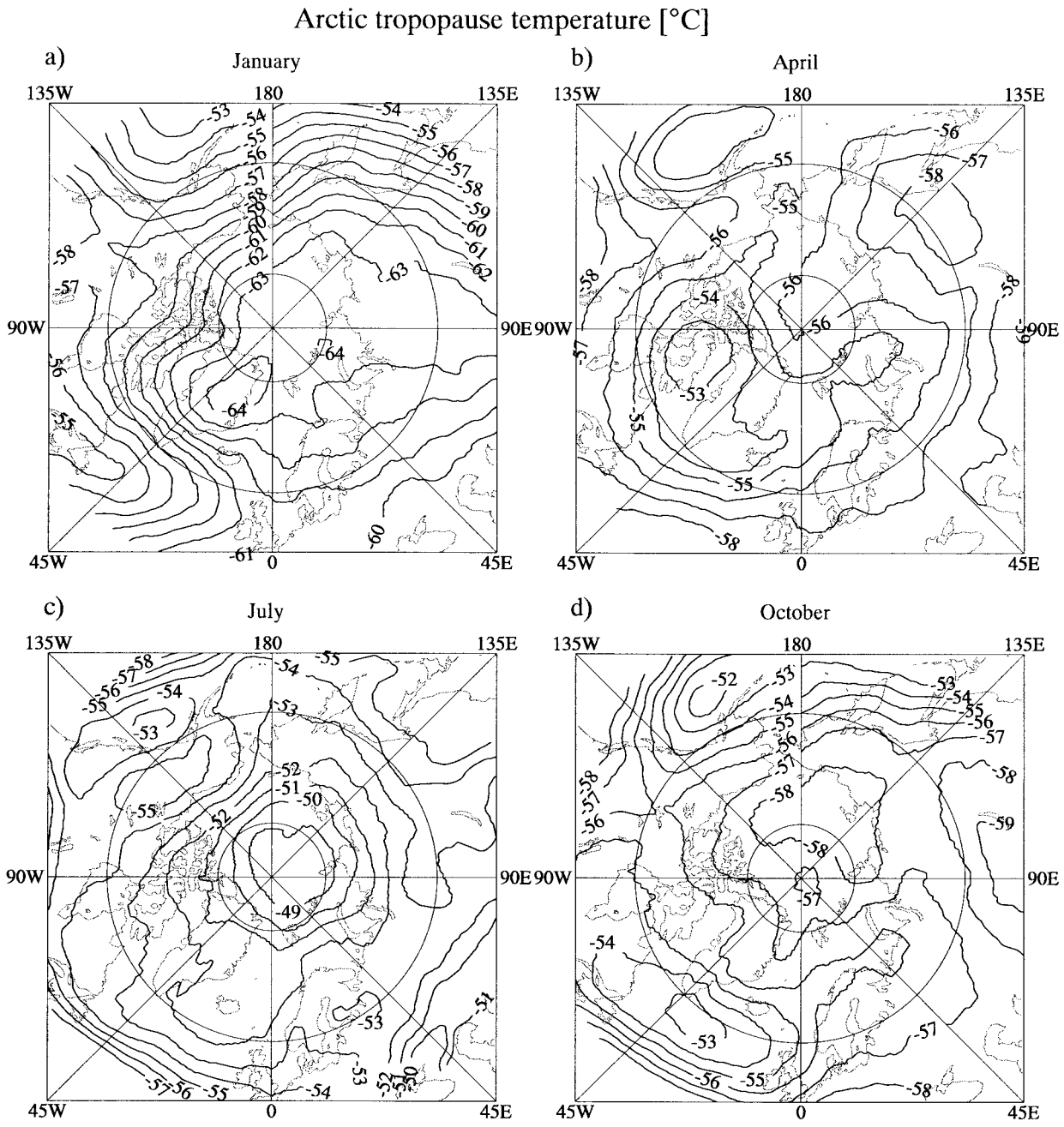


FIG. 4. Same as Fig. 3, but tropopause temperature. Contour interval is 1 K.

Over the rest of the Arctic, the tropopause pressure is generally between 260 and 290 hPa, and horizontal gradients are very weak. Toward the midlatitudes, the tropopause pressure decreases except for eastern Siberia where values above 300 hPa are reached off the Pacific coast. All in all, the pattern shows considerable zonal asymmetries with highest tropopause pressures (lowest tropopauses) in the large-scale Rossby wave troughs on the eastern side of the continents. Comparison with the December–January–February (DJF) field of HHB, who used the thermal criterion, reveals considerable differences over Europe and western Siberia. In these regions, the tropopause pressure computed by HHB is 10–25 hPa lower than that found in the present study. The DJF field shown by H98 for the dynamical tropopause is, however, much closer to the present results. We were able to reconstruct that these differences are due to the different tropopause criteria. As will be shown in section 7, the thermal criterion is not fully appropriate for Arctic winter.

In April, the tropopause pressure is significantly higher than in January throughout the Arctic. As will be

shown in the next section, the maximum of the annual cycle is reached in April in most parts of the Arctic. Local pressure maxima above 320 hPa are found over western Siberia and again over Canada. Toward the midlatitudes, however, the tropopause pressure tends to decrease between January and April. Correspondingly, meridional gradients are significantly stronger than in January. Unlike above, the differences between the present result and the corresponding MAM field of HHB are small and arise primarily from smoothing effects.

In July, meridional gradients are still quite strong with the tropopause pressure increasing towards the Pole, but the pattern is now relatively close to zonal symmetry. This apparently reflects the fact that Rossby wave activity is weakest in summer. Compared to April, the tropopause pressure has decreased both in polar regions and toward the midlatitudes. Until October, the tropopause pressure increases again, but the increase is much stronger in subpolar regions than near the Pole. Therefore, very weak gradients are present poleward of about 60°N. The differences between the thermal tropopause (HHB) and the dynamical tropopause are again small in summer and autumn.

Considering the annual cycle of the tropopause pressure, one finds a double wave with pressure maxima in spring and autumn and minima in summer and winter in a large part of the Arctic. Toward the midlatitudes, a single wave with a pressure maximum in winter and a minimum in summer prevails. The annual cycle will be discussed in more detail in the next section.

Tropopause temperature in January shows a large-scale minimum with temperatures between −63° and −64°C over Europe and western Siberia. It roughly coincides with the climatological location of the Arctic polar vortex. Weak local minima appear over Greenland and Franz-Josef-Land. Relatively high tropopause temperatures are found over Canada and in the Rossby wave trough off the Canadian Atlantic coast where the tropopause is low. It is interesting, however, that the western Pacific pressure maximum does not coincide with a temperature maximum. Rather, a temperature maximum is found over the eastern Pacific, near Alaska. This may possibly be explained with the air coming from Siberia being very cold in the whole troposphere and then being gradually warmed over the Pacific. The comparison with the DJF field of HHB reveals quite substantial differences. Throughout the Arctic, the HHB field is 3–6 K warmer, and the temperature minimum is located over the Arctic Ocean around 135°E. A part of this difference can be explained with the different methods of calculating the tropopause temperature. While HHB computed the tropopause temperature by interpolating the temperature between the adjacent model levels, the temperature gradients above or below the tropopause were extrapolated in the present study. As shown in Fig. 2d, interpolation leads to a significant warm bias. Another part of the difference is due to the fact that the DJF mean is substantially warmer than the January field (see also section 4, Fig. 7c).

In April, and also in October, the tropopause temperature is generally between −53° and −58°C, and meridional gradients are weak. In these months, the midlatitudes-to-pole gradient of the tropopause temperature reverses its direction. In summer, the tropopause is warmest near the Pole with a maximum between −48° and −49°C in July. The corresponding fields shown by HHB are again significantly warmer than those presented here. In these cases, the differences are primarily due to the different algorithms. Smoothing effects add to this in spring and autumn.

### *b. Antarctic tropopause*

Tropopause pressure and temperature for the SH are shown in Figs. 5 and 6. As will be shown in the following, there are several substantial differences between the two hemispheres, especially in winter and spring. In January, which has to be compared with July (NH), the tropopause pressure maximum is also located near the Pole, but it exhibits larger values (>330 hPa). Moreover, the meridional gradient is mainly concentrated to the regions equatorward of 60° latitude in the SH while it is more uniformly distributed in the Northern Hemisphere. In autumn (April), the tropopause pressure pattern differs little from the summer pattern except for the distribution of local maxima and minima over Antarctica, which is probably not very significant. Comparison with Fig. 3 shows that interhemispheric differences are weakest in autumn. In winter, however, things change dramatically. The meridional gradient of the tropopause pressure reverses its direction, and values below 230 hPa—almost 100 hPa less than in summer—are now found near the pole. Until October, there is little change except for a general increase of the tropopause pressure by 10–25 hPa. This means that there are two major differences in the annual cycle of the tropopause pressure between the Arctic and the Antarctic. First, a single wave with a pressure maximum in summer and a minimum in winter does not occur anywhere in the north polar region. The single wave that is typical for the northern midlatitudes has reversed sign, that is, a pressure minimum in summer and a maximum in winter. Second, differences between autumn and spring are much larger in the Antarctic than in the Arctic. A more detailed discussion of the annual cycles will be given in the next section. Apart from this, one observes that the fields in the Antarctic are closer to zonal symmetry than in the Arctic, especially in winter. This is due to the more symmetric orography and the resulting weaker Rossby wave activity.

Interhemispheric differences in tropopause temperature show similarities to pressure differences in several aspects. Again, the largest differences occur in winter and spring, and the fields are much closer to zonal symmetry in the Antarctic than in the Arctic. In summer,

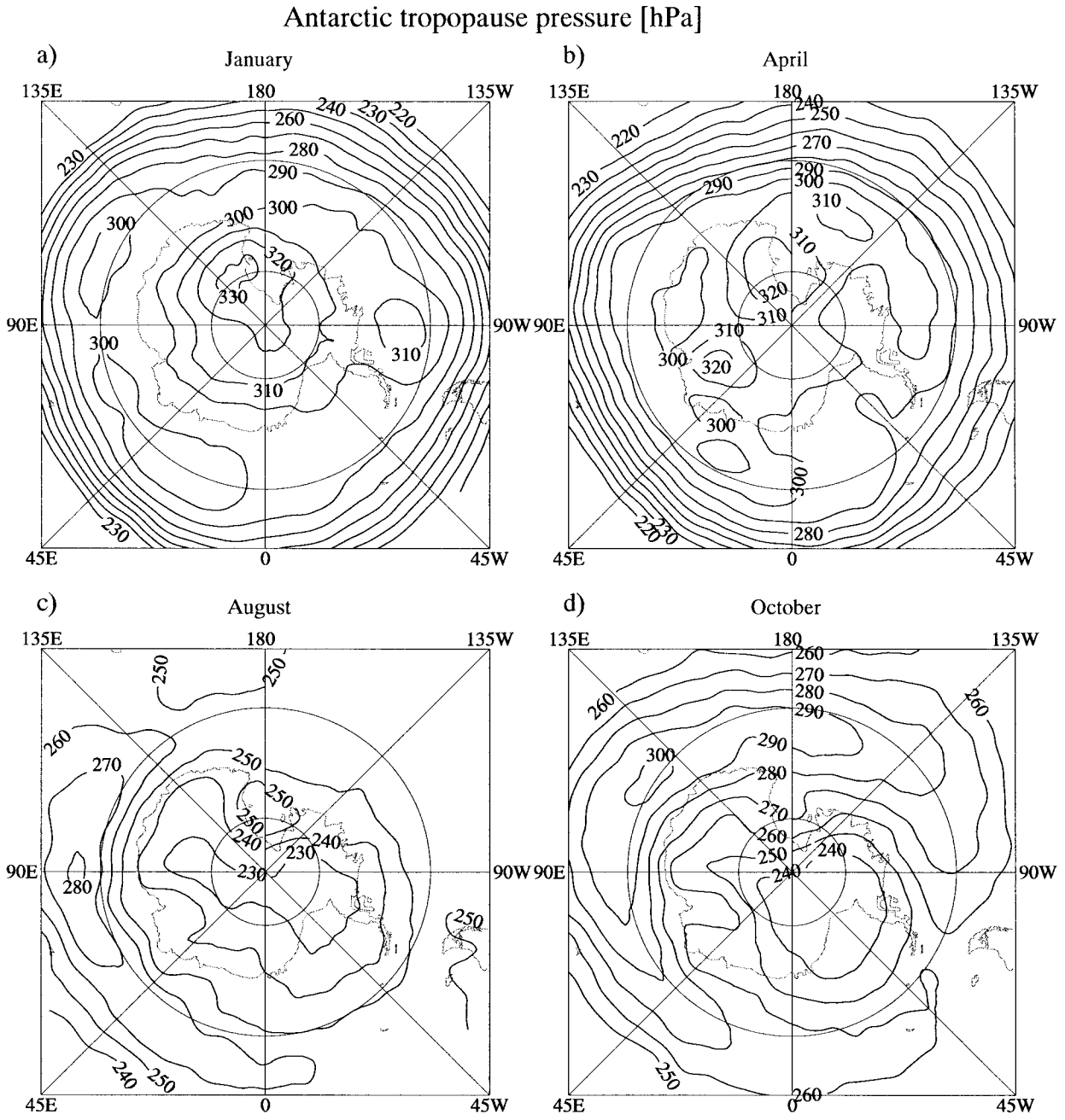


FIG. 5. Same as Fig. 3, but Antarctic tropopause pressure. In (c), Aug is displayed instead of Jul.

the overall temperatures are similar in both hemispheres, but meridional gradients mainly concentrate to the latitudes north of 60°S as they do for tropopause pressure. In autumn, temperature differences are still below 5 K, but meridional gradients and zonal symmetry are more pronounced in the Antarctic. However, the Antarctic tropopause is more than 10 K colder than the Arctic one in winter and spring. Correspondingly, Antarctic spring is about 10 K colder than Antarctic autumn while differences between April and October hardly exceed 2 K in the Arctic.

An explanation for these large interhemispheric differences can be found in the different strength and stability of the polar vortices that in turn depends on the Rossby wave activity in the midlatitudes. Rossby waves propagating into the stratosphere and breaking there act as a source of negative zonal momentum and drive the well-known stratospheric meridional circulation (e.g., Holton et al. 1995). The subsidence in the polar stratosphere connected with this circulation is, in the zonal mean, roughly twice as strong in the Arctic than in the Antarctic winter stratosphere (e.g., Rosenfield et al.

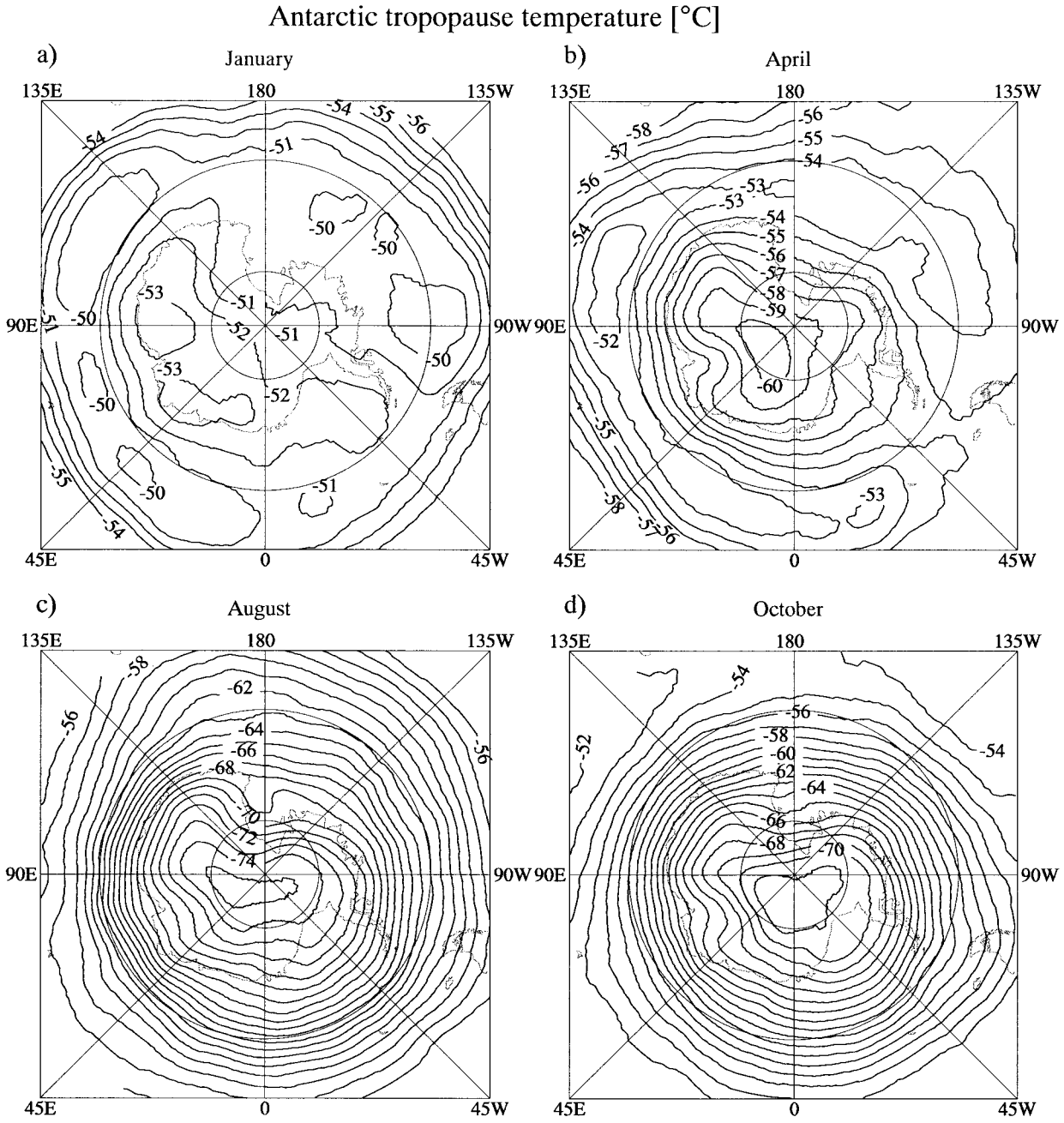


FIG. 6. Same as Fig. 5, but tropopause temperature. Contour interval is 1 K.

1987). Therefore, the Antarctic polar vortex is colder and more stable than the Arctic one. Moreover, the Arctic stratosphere is impacted by major stratospheric warmings while the Antarctic one is not. Major warmings are defined by a reversal of the meridional temperature and geopotential gradient between the Pole and 60° latitude at the 10-hPa level (Naujokat 1992). Climatologically, major warmings occur every second or third winter, and in most cases, they are accompanied by a significant temperature increase in the lower stratosphere, too (Naujokat and Labitzke 1993). Typically, major warmings start between mid-January and mid-February. Therefore, the climatological temperature minimum in the Arctic polar vortex is reached in the middle of January, well before solar heating sets in. In April, the polar vortex has already disappeared in most years. Over Antarctica, however, temperatures continue to fall as long as the polar vortex lies in the dark, leading to a climatological temperature minimum at the end of August. Moreover, since the breakup of the Antarctic polar vortex is hardly supported by large-scale subsidence, it takes until the middle of November—almost

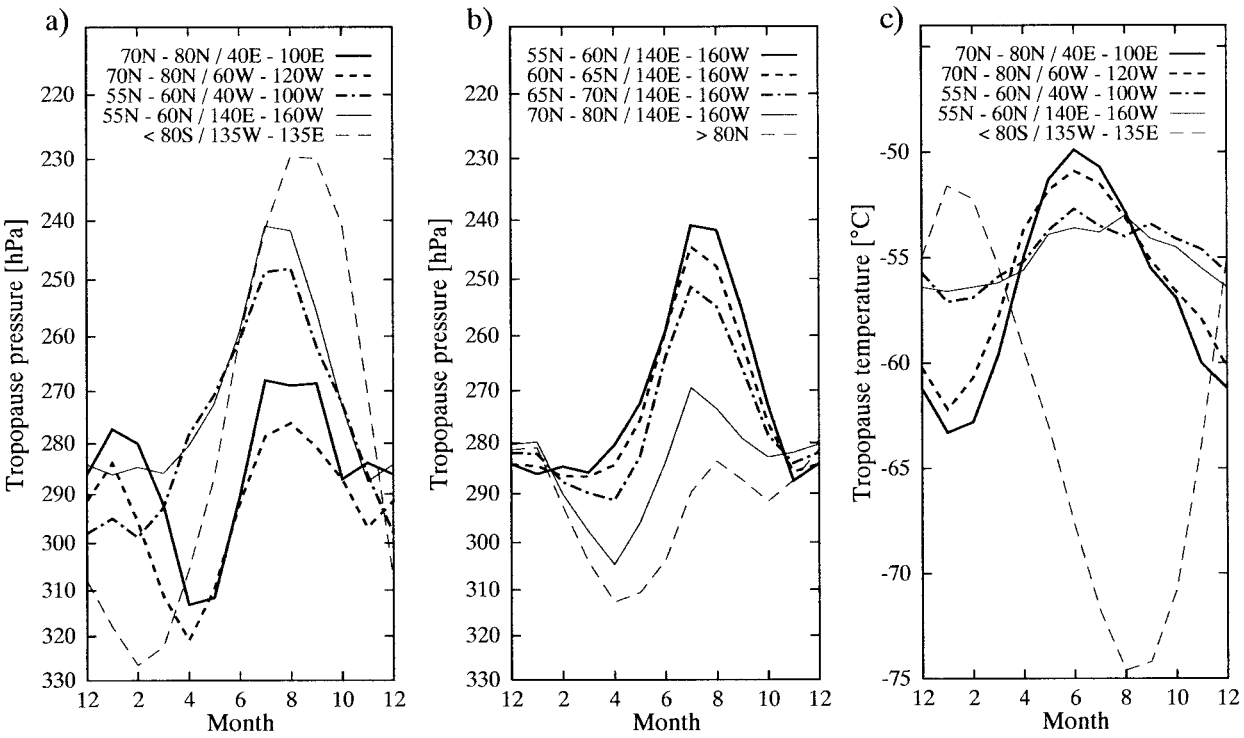


FIG. 7. Annual cycle of (a), (b) tropopause pressure, (c) tropopause temperature for selected regions.

two months longer than in the NH—for the polar vortex to be dissolved. In essence, October can be taken as a winter month in the Antarctic, while April is marked by the transition from winter to summer in the Arctic.

## 6. The annual cycle of the tropopause

It can be inferred from Figs. 3 and 5 that the annual cycles of polar tropopause pressure can be classified into three different patterns. A single wave with highest tropopause pressure in winter and lowest in summer is typical for the midlatitudes and for the subpolar parts of eastern Siberia and North America. Northern Europe, western Siberia, and, generally, high Arctic latitudes exhibit a double wave with pressure maxima in spring and autumn and pressure minima in summer and winter. Finally, a single wave with maximum tropopause pressure in summer and minimum pressure in winter is found over the whole of Antarctica, with the amplitude increasing toward the South Pole. Transition zones without a distinct annual cycle are located in the southern midlatitudes around 50°S and in the subpolar parts of Europe.

Typical examples for the three patterns are displayed in Fig. 7a. The largest amplitude is found over central Antarctica with a maximum–minimum difference of about 100 hPa. Note that the extrema are attained in February and August–September. The single waves found in the subpolar parts of eastern Siberia and Canada–Alaska have a maximum–minimum difference of about 50 hPa, half as much as in central Antarctica. The summer minimum is attained in July–August, and the winter maximum is quite broad, especially in eastern Siberia where the tropopause pressure is almost constant between November and March. Even lower pressure amplitudes (~30–40 hPa) are found at high northern latitudes where a double wave prevails. The primary pressure maximum is generally found in April in these regions, and the primary minimum is reached in July or August except for the region >80°N (Fig. 7b) where the tropopause pressure is lowest in December and January. The difference between the secondary maximum, which is attained in October or November, and the local minimum in January is generally weak. The transition from the single wave in subpolar regions to the double wave at high latitudes is demonstrated in Fig. 7b. While there are little differences in winter, the tropopause pressure increases in spring at high latitudes while it decreases in subpolar regions. In summer, a strong meridional gradient is evident, which has already been mentioned in the discussion of Fig. 3.

The tropopause temperature curves for the regions displayed in Fig. 7a are given in Fig. 7c. It is clearly evident that the regions with similar pressure patterns have also similar tropopause temperatures. The subpolar regions with a single pressure wave are marked with an almost constant tropopause temperature, the summer–winter difference amounting to only 3 K. At high northern latitudes, a temperature amplitude of 11–13 K is found, and an impressive value of 23 K is attained over

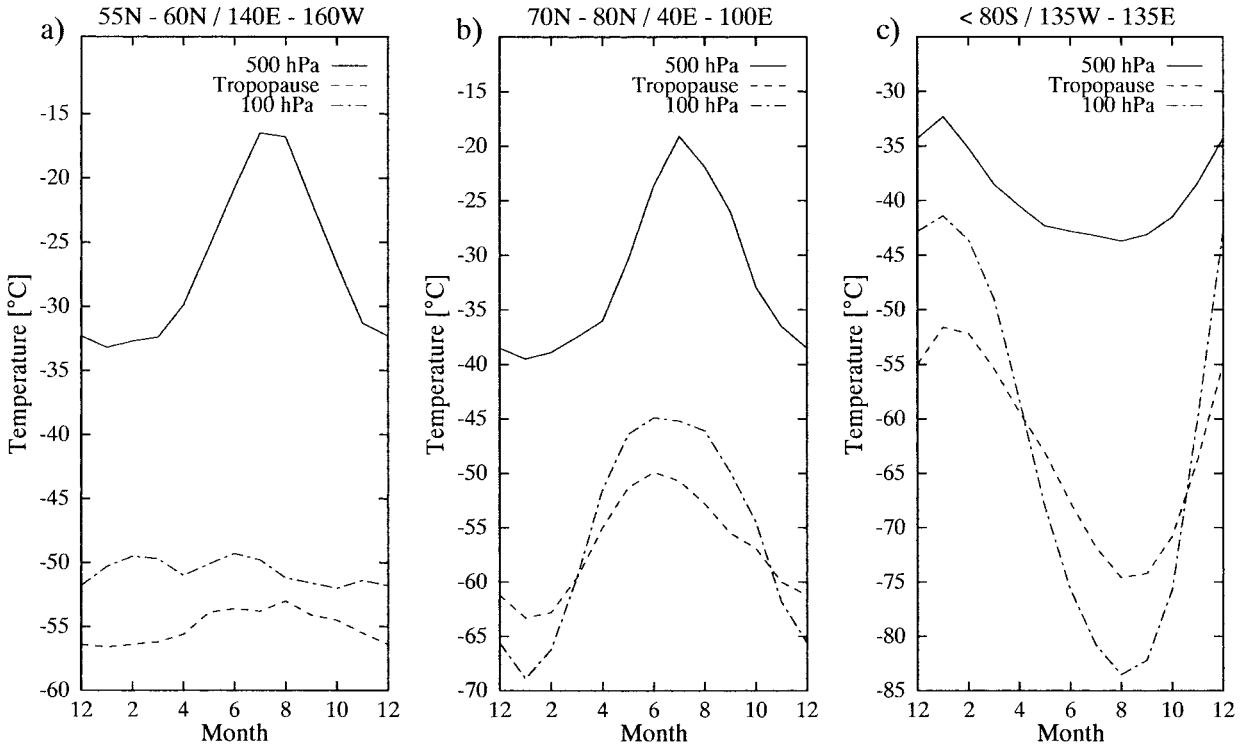


FIG. 8. Annual cycle of 500-hPa temperature, tropopause temperature, and 100-hPa temperature for three regions.

central Antarctica. Note that the temperature minimum is reached in January in the Arctic while it is reached in August in the Antarctic. As mentioned above, these differences can be traced back to the differences in dynamical heating of the stratosphere.

In the following, it will be shown that the annual cycles of the tropopause pressure are closely related to the temperature difference between the midtroposphere and the lower stratosphere. Suppose, for example, that the surface temperature and the tropospheric temperature gradient are given and that the temperature of the stratosphere varies. Then, a cold stratosphere will be associated with a high tropopause (low tropopause pressure), and a warm stratosphere will correspond to a low tropopause (high tropopause pressure). A similar argument has already been proposed by Möller (1938). Of course, tropospheric temperatures are not constant throughout the year, but in a more general sense, one may expect that the tropopause pressure varies with the temperature difference between the midtroposphere and the lower stratosphere, for example, between 500 and 100 hPa. A large (small) temperature difference is then expected to be associated with a low (high) tropopause pressure.

Comparison of Figs. 7 and 8 reveals that this is indeed the case. In subpolar eastern Siberia (55°–60°N, 140°E–160°W; Fig. 8a), the 100-hPa temperature ($T_{100}$) is almost constant throughout the year while the 500-hPa temperature ($T_{500}$) has a distinct summer maximum. Therefore, $T_{500} - T_{100}$ is larger in summer than in winter, corresponding to a tropopause pressure minimum in summer and a maximum in winter. Interestingly, this relation even holds for the months of November until March where both the tropopause pressure and $T_{500} - T_{100}$ are almost constant. Over central Antarctica (Fig. 8c), the temperature amplitude is much larger in 100 hPa than in 500 hPa, yielding a maximum of $T_{500} - T_{100}$ in August and a minimum in February. As the tropopause pressure extrema are attained in August (min) and in February (max), expectations are again met. Finally, northwestern Siberia (70°–80°N, 40°–100°E; Fig. 8b) is to be considered. Although the temperature ranges in 500 and 100 hPa have similar amplitudes, they are by no means parallel. In 500 hPa, there is a broad temperature minimum in winter and a sharp maximum in summer. On the other hand, a sharp minimum in winter and a broad maximum in summer are found in 100 hPa. As a result, $T_{500} - T_{100}$ attains two maxima in January and July and two minima in April and October, again fitting the tropopause pressure extrema.

This excellent correlation between $T_{500} - T_{100}$ and the tropopause pressure can be used to identify one important mechanism influencing the location of the polar tropopause. Comparing the temperature curves displayed in Fig. 8, one finds that it is primarily the $T_{100}$ cycle that exhibits large regional differences. Simulations with a radiative-convective model, which will be reported in a separate paper, indicate that these differences are mainly due to differences in the dynamical heating of the lower stratosphere. This suggests that the

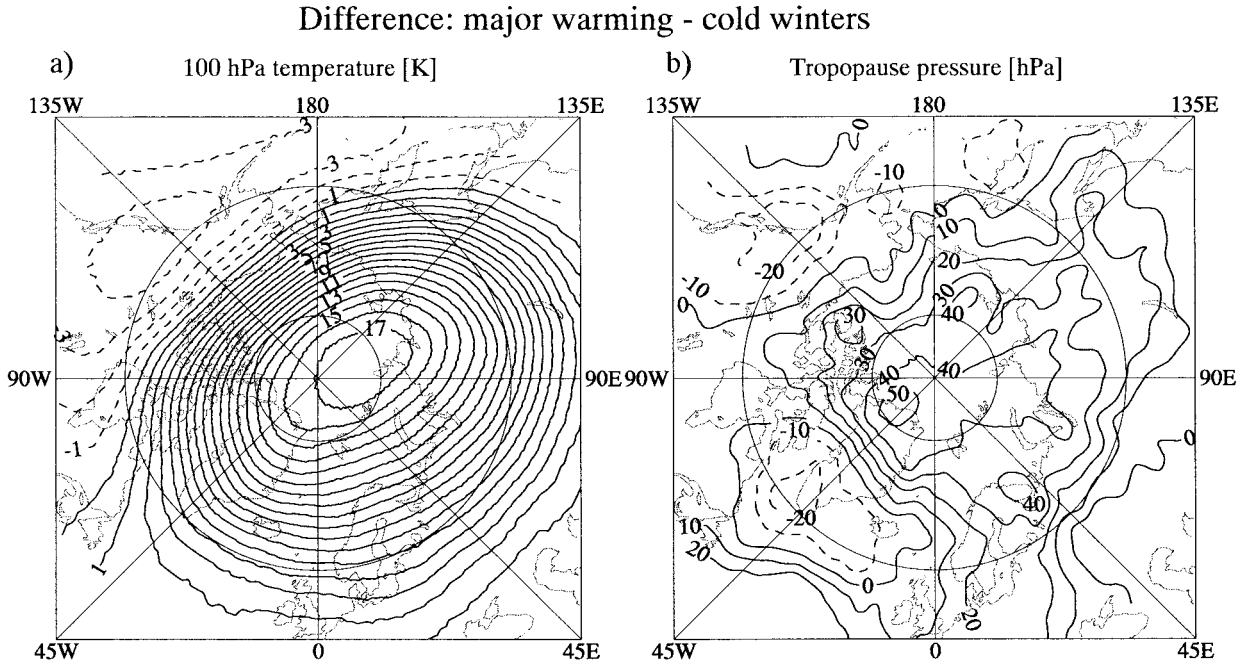


FIG. 9. Difference in (a) 100-hPa temperature and (b) tropopause pressure between Arctic winters influenced by major stratospheric warmings and cold winters. Contour intervals are 1 K and 10 hPa, respectively; negative isolines are dashed.

dynamical heating, which is related to the stratospheric meridional circulation (see section 5b), is one of the factors determining the height of the polar tropopause. Some evidence for the influence of dynamical heating can also be gained directly from the data. A comparison of winters, in which a major stratospheric warming occurred, with cold winters (with respect to the lower stratosphere), provides a way to isolate the effects of dynamical heating. Using the statistics of Naujokat and Labitzke (1993) and half-monthly means of $T_{100}$ from the ERA data, a class of seven major warming-influenced half months and a class of fourteen half months marked with a strong, cold polar vortex have been defined. The major warming class comprises the first half of February 1981 and 1991, January and the first half of February 1985, the second half of December 1987 and the first half of January 1988. The differences between the two classes (warm–cold) are displayed in Fig. 9. As can be seen in Fig. 9a, the $T_{100}$ differences reach up to 17 K near the pole. The corresponding tropopause pressure differences are shown in Fig. 9b. Over a large fraction of the Arctic, values between 30 and 50 hPa are found, emphasizing the large influence dynamical heating can have. Of course, this behavior is consistent with the simple geometric consideration given above that a warm stratosphere should be associated with high tropopause pressure. It should be noted that the differences shown in Fig. 9b are highly significant. The standard deviation of monthly mean tropopause pressures from year to year, computed as

$$\sigma^M_{p_{\mathrm{TP}}} := \sqrt{\frac{1}{14}\sum_{y=1979}^{1993}(\overline{p}^M_{\mathrm{TP}_y} - \overline{p}^M_{\mathrm{TP}})^2},$$

where $\overline{p}^M_{\mathrm{TP}_y}$ is the monthly mean tropopause pressure of a single year and $\overline{p}^M_{\mathrm{TP}}$ is the monthly mean pressure of all years (as displayed in Figs. 3 and 5), ranges between 15 and 20 hPa in Arctic winter (not shown). Thus, the two classes defined above are about two standard deviations apart.

## 7. Comparison between thermal and dynamical tropopause

All results presented in the preceding two sections refer to the dynamical (3.5 PVU) tropopause. In this section, the differences between the thermal and the dynamical tropopause are discussed. Generally, it can be stated that both tropopause definitions yield similar results except for winter. In Arctic winter, differences are weak over eastern Siberia and Canada only. However, the thermal tropopause pressure is 10–20 hPa lower than the dynamical one over northern Europe and western Siberia, that is, in the polar vortex region. This confirms that the differences between our January tropopause pressure field and the DJF field presented by HHB are primarily due to the different tropopause criteria. Even stronger differences are found in Antarctic winter and Antarctic spring. In August, the thermal tropopause pressure is below 170 hPa over central Antarctica (Fig. 10a), corresponding to a thermal–dynamical difference of more than 60 hPa (Fig. 10b).

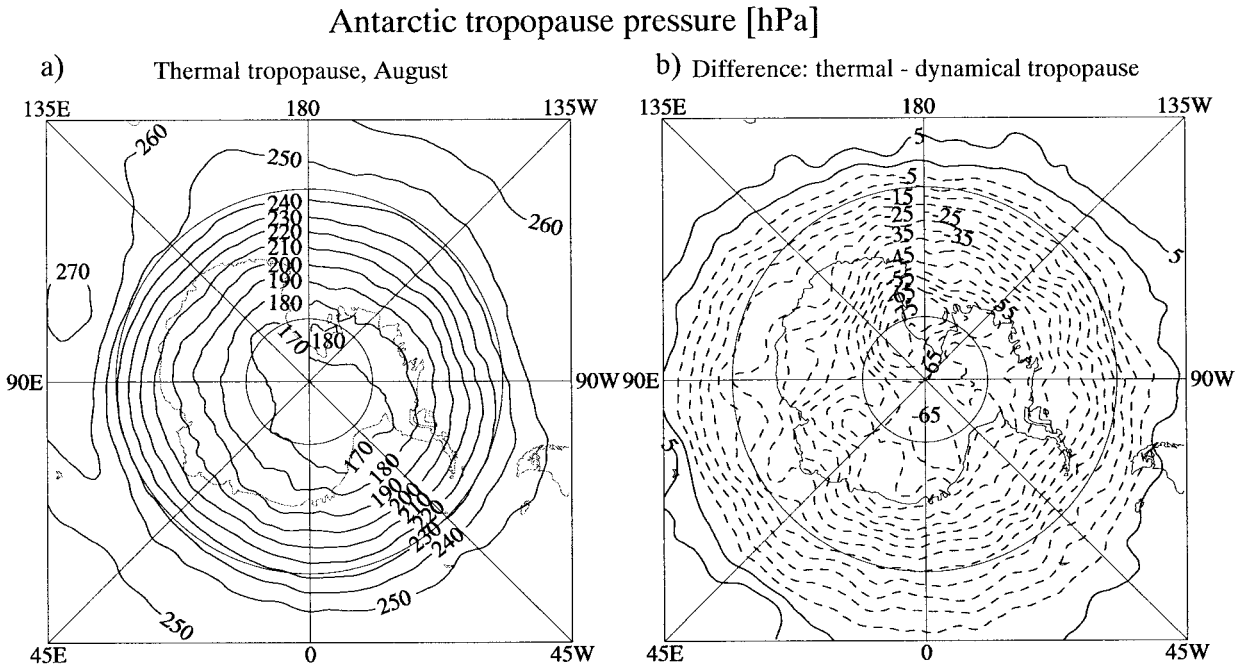


FIG. 10. (a) Thermal tropopause pressure, Antarctica, Aug. Contour interval is 10 hPa. (b) Difference between thermal tropopause pressure and dynamical tropopause pressure (i.e., between Figs. 10a and 5c). Contour interval is 5 hPa; negative isolines are dashed.

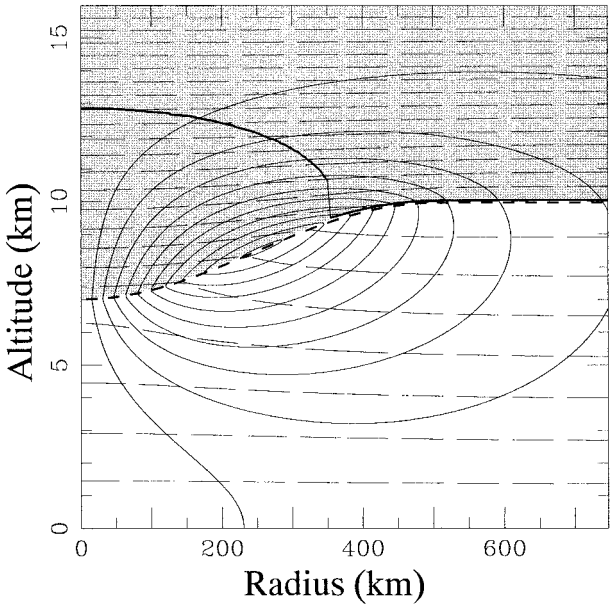


FIG. 11. Result of a PV inversion for typical Antarctic winter conditions. The thermal tropopause is marked by the thick solid line, dashed lines denote potential temperature (contour interval 5 K), and thin solid lines denote tangential wind speed (relative units). Gray shading denotes PV $> 3.5$ PVU, thus the lower boundary of the gray-shaded area is the dynamical tropopause. The downward displacement of the tropopause between radius $r = 0$ and $r = 500$ km specifies an upper-tropospheric cyclone.

A closer investigation reveals that these large differences are primarily due to a too low static stability in the lower stratosphere. It has been found that the mean vertical temperature gradient in the Antarctic lower stratosphere is below $-1.0$ K km$^{-1}$ between June and October. In July and August, it is even below $-1.5$ K km$^{-1}$. Thus, it is not surprising that the application of the thermal criterion is problematic in Antarctic winter. More precisely, it depends on synoptic-scale conditions whether the thermal criterion yields a meaningful tropopause or not. As can easily be reproduced with the technique of PV inversion, a thin, very stable layer is typically present above upper-tropospheric anticyclones, while the lower stratosphere is less stable than in its background state within and above cutoff lows (e.g., Hoskins et al. 1985). In anticyclonic cases, it can therefore be expected that both tropopause criteria yield the same results, but in cyclonic cases, the thermal criterion may diagnose a substantially lower tropopause pressure than the dynamical one.

In order to illustrate this point, a PV inversion has been performed for a cyclonic disturbance embedded in background conditions typical for Antarctic winter [see Wirth (2000) for a description of the algorithm]. Tropospheric and stratospheric temperature gradients are assumed to be $-6.5$ and $-1.0$ K km$^{-1}$, respectively, and the cyclone is prescribed as a cos$^2$-shaped displacement of the tropopause with a radius of 500 km and a peak displacement of 3 km. Axisymmetry and gradient wind balance are assumed for the inversion. The result is displayed in Fig. 11. While the dynamical tropopause,

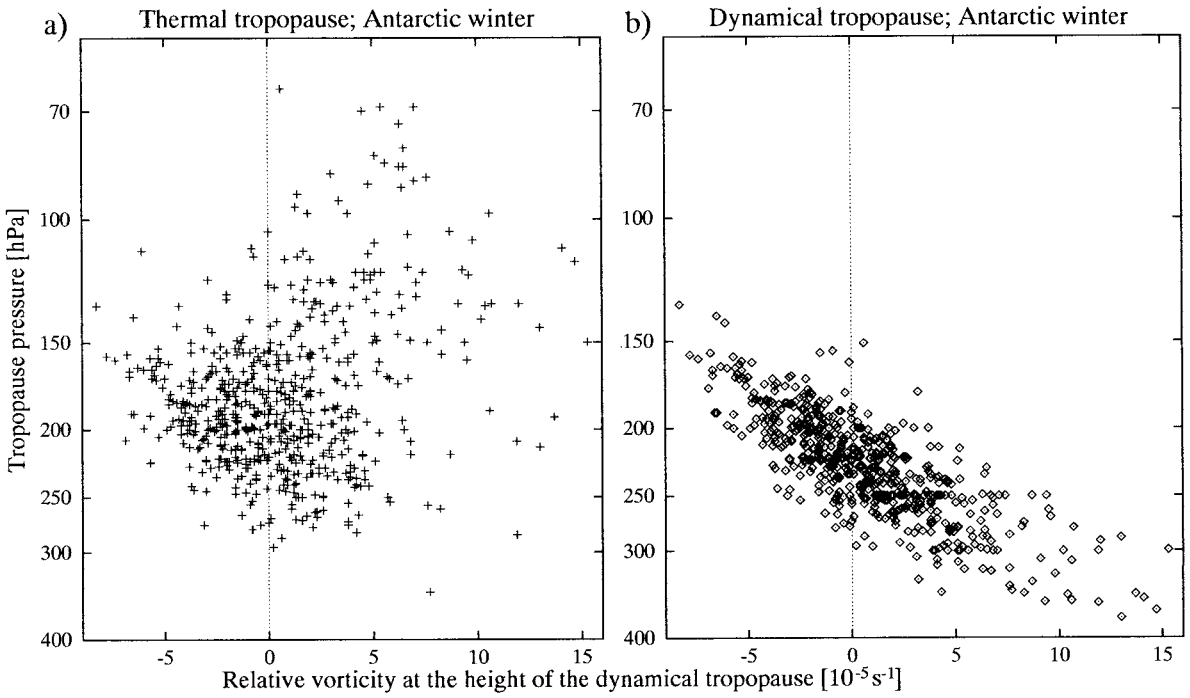


FIG. 12. (a) Thermal and (b) dynamical tropopause pressure (hPa) obtained from the radiosonde data for central Antarctica for the months Jul–Oct. The relative vorticity (in $10^{-5}$ $s^{-1}$) is multiplied by $-1$ so that positive values denote cyclonic vorticity.

denoted by the lower boundary of the gray-shaded area, is displaced downward in the cyclone, the thermal tropopause, denoted by the thick solid line, is displaced upward. Due to the cyclone-induced destabilization of the lower stratosphere, the thermal criterion is not met at the height of the dynamical tropopause but several kilometers higher up. In the cyclone center, thermal and dynamical tropopauses are 6 km apart.

A similar behavior can be inferred from data. Figure 12 shows thermal and dynamical tropopause pressures obtained from the radiosondes of central Antarctica (South Pole, Vostok and Halley Base) for the months of July to October. They are displayed as a function of relative vorticity at PV-tropopause level, normalized with the sign of the Coriolis parameter so that positive values correspond to cyclonic influence. It can be seen that the PV tropopause pressure increases continuously with relative vorticity. This is consistent with other observations and theoretical considerations (e.g., Hoskins et al. 1985). However, the opposite is the case for the thermal tropopause. Apart from strong scattering, the thermal tropopause pressure tends to decrease with increasing cyclonic influence. For anticyclonic cases, there is a good correspondence between both tropopause criteria, but under cyclonic influence, the thermal tropopause is found to be up to 10 km above the dynamical tropopause.

Thus, it can be concluded that the thermal criterion is not appropriate for polar winter. Due to the low static stability of the lower stratosphere, the thermal criterion does not yield a physically meaningful tropopause under cyclonic influence. In many cases, the thermal tropopause corresponds to PV values of 10 PVU or more (not shown). Moreover, the thermal criterion is very sensitive to little changes in the temperature profile. As shown in Fig. 2c, the correspondence between radiosonde-derived tropopauses and ERA-derived tropopauses is far worse in Antarctic winter than anywhere else. Tests with a lower threshold value (e.g., $-3$ K $km^{-1}$) revealed some improvement in Antarctic winter, but severe problems occurred in Canadian and eastern Siberian winter where the vertical temperature gradient may be around $-3$ K $km^{-1}$ throughout the troposphere. Therefore, a modification of the thermal criterion cannot be regarded as meaningful. With a possible exception of conserved trace gases (e.g., ozone; see Bethan et al. 1996), there appears to be no alternative to the PV-based tropopause definition in polar winter.

## 8. The sharpness of the tropopause

Finally, the sharpness of the polar tropopause shall be investigated. According to Wirth (2000), the tropopause sharpness is defined as the change in vertical temperature gradient across the tropopause, that is,

$$S_{\mathrm{TP}} := \frac{T_{\mathrm{TP}+\Delta z} - T_{\mathrm{TP}}}{\Delta z} - \frac{T_{\mathrm{TP}} - T_{\mathrm{TP}-\Delta z}}{\Delta z},$$

with $\Delta z = 1$ km, for example. Since both $\gamma_{+\Delta z} = (T_{\mathrm{TP}+\Delta z} - T_{\mathrm{TP}})/\Delta z$ and $\gamma_{-\Delta z} = (T_{\mathrm{TP}} - T_{\mathrm{TP}-\Delta z})/\Delta z$ exhibit distinct annual cycles and regional differences, these quantities

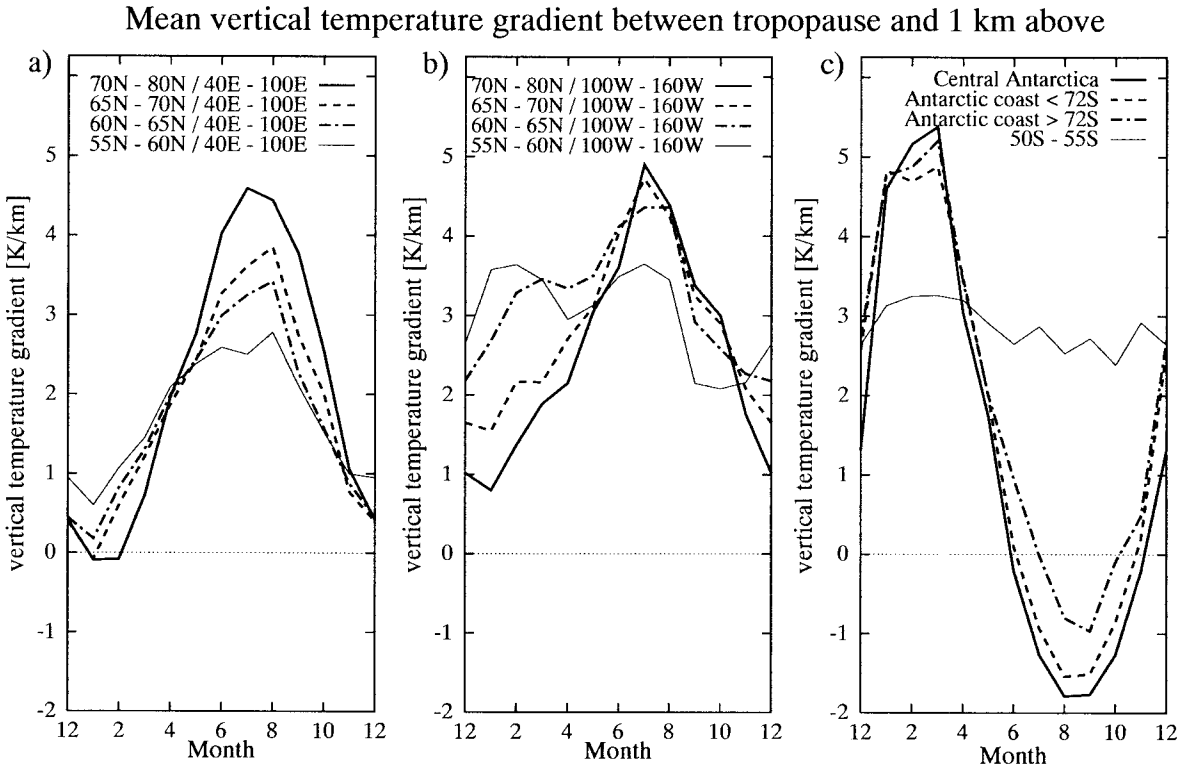


FIG. 13. Annual cycle of the mean vertical temperature gradient between the tropopause and 1 km above for selected regions.

will be discussed separately before combining them to yield the tropopause sharpness.

Since the vertical resolution of the ERA data is not sufficient to determine the tropopause sharpness, temperature gradients are taken exclusively from radiosonde data. Moreover, the investigation is restricted to the dynamical tropopause because the thermal criterion is not appropriate for polar winter (see above). As in section 4, certain geographical regions are put together to clarify the regional differences of tropopause sharpness. In the Northern Hemisphere, we consider four latitude belts (55°–60°N, 60°–65°N, 65°–70°N, and 70°–80°N) and seven longitude sections, two of which are discussed in the following (western Siberia; 40°–100°E and Alaska–Canada; 100°–160°W). In the SH, the sparsity of radiosonde stations allows only for a division into four regions, namely 50°–55°S, 62°–72°S, Antarctic coast <72°S, and central Antarctica.[2] Note that there are no stations between 55° and 62°S.

The mean vertical temperature gradients between the tropopause and 1 km above ($\gamma_{+1}$) are displayed in Fig. 13. Generally, it can be stated that $\gamma_{+1}$ is larger in summer than in winter and that the amplitude of this annual cycle increases toward the Poles. As for tropopause pressure and temperature, the largest annual cycle is found over central Antarctica where $\gamma_{+1}$ exceeds $+5$ K km$^{-1}$ in summer and is close to $-2$ K km$^{-1}$, the threshold value of the thermal criterion, in winter. At high Arctic latitudes, summer values are close to Antarctic values while $\gamma_{+1}$ hardly falls below 0 K km$^{-1}$ in winter. This is consistent with the fact that the thermal criterion does a better job in Arctic winter than in Antarctic winter. Moreover, distinct zonal differences are present in the Arctic winter. In the polar vortex region (Fig. 13a), $\gamma_{+1}$ ranges between 0 and $+1.0$ K km$^{-1}$ while it ranges between $+1.0$ and $+3.5$ K km$^{-1}$ in the Aleutian high region (Fig. 13b). The remaining longitude sections range between these values, with eastern Siberia being close to Alaska, middle Siberia being close to western Siberia and Europe being about half way in between. In summer, zonal differences are weaker, but $\gamma_{+1}$ is still larger over Canada and Alaska than over western Siberia. However, the remaining regions behave differently from winter. $\gamma_{+1}$ is even larger in Europe than in Canada and is even lower in middle and eastern Siberia than in western Siberia. Finally, note the abrupt change between the region 50°–55°S and the Antarctic coast. Although there are very few radiosonde stations in the southern hemisphere, there is clear evidence that the meridional gradient of the annual $\gamma_{+1}$-cycle is far stronger in the Antarctic than in the Arctic.

The mean vertical temperature gradients between the

[2] The station Halley Base (89022; 75°S, 26°W) is put together with the central Antarctic stations although it is a coastal station because its tropopause properties are similar to central Antarctica (see Figs. 5 and 6).

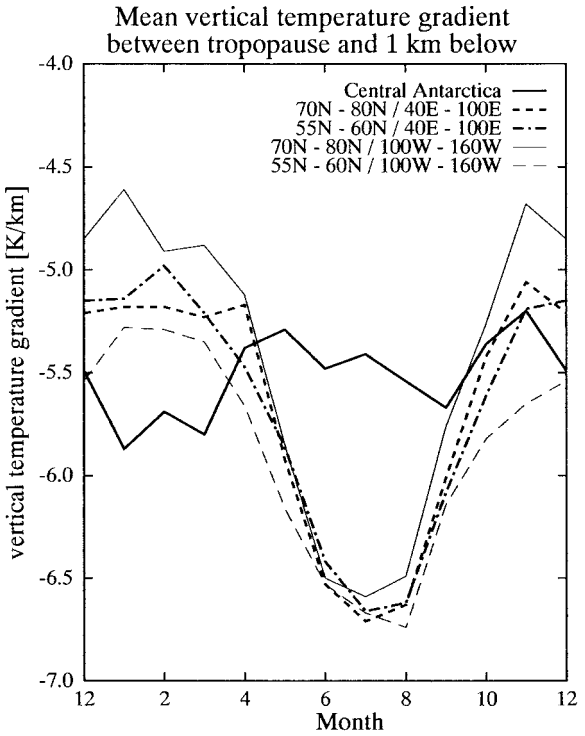


FIG. 14. Annual cycle of the mean vertical temperature gradient between the tropopause and 1 km below for selected regions.

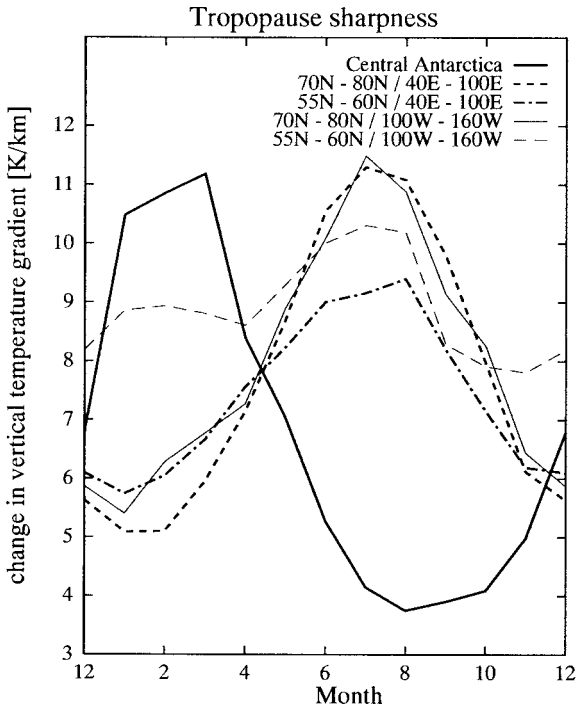


FIG. 15. Annual cycle of the tropopause sharpness for selected regions.

tropopause and 1 km below ($\gamma_{-1}$) show weaker annual cycles and regional differences than $\gamma_{+1}$, but they are still worth to be discussed shortly. Some selected regions are displayed in Fig. 14. First, it may be noted that the annual cycle of $\gamma_{-1}$ is weaker in the Antarctic than in the Arctic. This is also valid for the regions not shown here. In the Arctic, $\gamma_{-1}$ is generally lower in summer than in winter, indicating that the troposphere is more stably stratified in winter. There are almost no regional differences in Arctic summer, $\gamma_{-1}$ being very close to the standard atmosphere value of $-6.5$ K km$^{-1}$, but there are moderate differences in winter. The highest values ($\approx -4.5$ K km$^{-1}$) are found in Canada–Alaska poleward of 70°N and in middle and eastern Siberia between 55° and 70°N. The lowest values ($\approx -5.7$ K km$^{-1}$) are found in Europe (not shown).

It follows that the annual cycle and the regional differences of the tropopause sharpness (Fig. 15) arise primarily from $\gamma_{+1}$. Consequently, the tropopause sharpness is substantially higher in summer than in winter with the amplitude increasing toward the Poles. The main effect of $\gamma_{-1}$ is that the summer maximum of tropopause sharpness is slightly higher at high northern latitudes than over central Antarctica although the opposite is the case for $\gamma_{+1}$. It should be mentioned that the synoptic-scale variability of tropopause sharpness is at least as large as its annual cycle. As mentioned in the previous section, the tropopause sharpness is much higher over upper-tropospheric anticyclones than within cutoff lows.

## 9. Summary

The polar and subpolar tropopause has been investigated using the ECMWF Reanalysis (ERA) data from 1979 to 1993 and radiosonde data from 1989 to 1993. Both the thermal and the dynamical (3.5 PVU) tropopause have been computed from each dataset. The tropopauses calculated from the radiosonde data have been used to validate the tropopauses calculated from the ERA data and to investigate the sharpness of the tropopause, which requires high vertical resolution. The validation revealed that the ERA data are suited very well for this study. The uncertainties in the determination of the tropopause pressure are negligible compared to typical regional differences, and the warm bias in the tropopause temperature arising from the low vertical resolution of the ERA data can be overcome by extrapolating the temperature gradient below or above the tropopause.

A central result from this study is that the annual cycle of polar tropopause pressure can be classified into three different patterns. A single wave with a tropopause pressure maximum in winter and a minimum in summer is found in the subpolar parts of eastern Siberia and North America. A double wave with pressure maxima in spring and autumn and minima in summer and winter is typical for northern Europe, western Siberia, and gen-

erally for high Arctic latitudes. Finally, Antarctica exhibits a reversed single wave with a pressure maximum in summer and a minimum in winter. Tropopause temperatures are generally highest in summer and lowest in winter, but the amplitude of their annual cycles shows large differences. It is lowest in those regions that exhibit the first pressure pattern (single pressure maximum in winter) and largest in the Antarctic. A comparison between the tropopause pressure and the temperatures in 500 and 100 hPa reveals that the tropopause pressure is closely related to the temperature difference between 500 and 100 hPa or, more generally, between the midtroposphere and the lower stratosphere. A large temperature difference then corresponds to a low tropopause pressure and a small temperature difference to a high tropopause pressure.

The differences between the thermal tropopause and the dynamical tropopause are weak except for polar winter. In Arctic winter, they are weak only in the Aleutian high region but moderate in the polar vortex region (Europe, western Siberia). The by far largest differences occur in Antarctic winter where the thermal tropopause pressure is about 60 hPa lower than the dynamical tropopause pressure. These differences can be traced back to the low static stability of the lower stratosphere in Antarctic winter. Since the mean vertical temperature gradient between the (dynamical) tropopause and the 100-hPa level is close to $-2$ K km$^{-1}$, that is, the threshold value of the thermal criterion, the thermal criterion is not appropriate for Antarctic winter.

A quantity that is closely related to the mean static stability of the lower stratosphere is the sharpness of the tropopause, that is, the change in vertical temperature gradient across the tropopause. Its annual cycle and its regional differences are primarily determined by the mean temperature gradient above the tropopause since it varies much more strongly than the gradient below the tropopause. Generally, the tropopause sharpness is higher in summer than in winter with the summer–winter difference increasing toward the Poles. In winter, the lowest tropopause sharpness is attained in the Antarctic, being accompanied with the failure of the thermal criterion. In the Arctic, the tropopause is sharper in the Aleutian high region than in the polar vortex region. The synoptic-scale variability of the tropopause sharpness will be addressed in detail in a future paper.

*Acknowledgments.* This study is part of the first author's Ph.D. thesis that was written at the University of Munich under the guidance of Joe Egger. The work was supported by the German Science Foundation (Deutsche Forschungsgemeinschaft, DFG). Many thanks are due to Volkmar Wirth for helpful discussions and for providing the PV inversion program. The German Weather Service (Deutscher Wetterdienst, DWD) is acknowledged for providing the radiosonde data. The ERA data were kindly provided by the ECMWF within the special project, ''The climatology of the global tropopause.''

## APPENDIX A

### Determination of the Thermal Tropopause from the ERA Data

The thermal tropopause is determined as follows. First, the vertical temperature gradient $\partial T/\partial z$ is calculated between each two adjacent model levels (indices $i$ and $i + 1$, respectively) by approximating $(\partial T/\partial z)_{i+1/2} := (T_{i+1} - T_i)/(z_{i+1} - z_i)$. This value is assigned to the mean geometric height of the model levels $z_{i+1/2} := (z_i + z_{i+1})/2$, corresponding to centered differences. Centered differencing was also used by HHB, but these authors apparently computed the differences at full model levels, leading to a smoothing of the vertical gradients. In order to exclude a possible surface inversion, the search starts at about 2000 m above ground. The search ends at 90 hPa because even lower tropopause pressures are certainly not meaningful in the polar regions (of course, a lower value would have to be used at low latitudes). Then, the lowest level that fulfills $(\partial T/\partial z)_{i+1/2} \geq -2$ K km$^{-1}$ and $(\partial T/\partial z)_{i-1/2} < -2$ K km$^{-1}$ is determined, and the tropopause height is set to

$$z_{\mathrm{TP}} = z_{i-(1/2)} + \frac{\gamma_{\mathrm{TP}} - \left(\frac{\partial T}{\partial z}\right)_{i+(1/2)}}{\left(\frac{\partial T}{\partial z}\right)_{i+(1/2)} - \left(\frac{\partial T}{\partial z}\right)_{i-(1/2)}}(z_{i+(1/2)} - z_{i-(1/2)}), \tag{A1}$$

where $\gamma_{\mathrm{TP}} = -2$ K km$^{-1}$ is the threshold value of the thermal criterion. Equation (A1) is identical to the method used by HHB, that is, the vertical temperature gradient is assumed to vary linearly with $z$ in the tropopause region. The tropopause pressure is calculated under the assumption $z \sim \ln p$

$$p_{\mathrm{TP}} = \begin{cases} p_i \exp\left[\ln\left(\frac{p_{i+1}}{p_i}\right)\frac{z_{\mathrm{TP}} - z_i}{z_{i+1} - z_i}\right], & \text{if } z_{\mathrm{TP}} > z_i \\ p_i \exp\left[\ln\left(\frac{p_i}{p_{i-1}}\right)\frac{z_{\mathrm{TP}} - z_i}{z_i - z_{i-1}}\right], & \text{if } z_{\mathrm{TP}} < z_i, \end{cases} \tag{A2}$$

and the tropopause temperature is computed by extrapolating the temperature gradient below the tropopause or above the tropopause

$$T_{\mathrm{TP}} = \begin{cases} T_i + \left(\frac{\partial T}{\partial z}\right)_{i-(1/2)}(z_{\mathrm{TP}} - z_i), & \text{if } z_{\mathrm{TP}} > z_i \\ T_i + \left(\frac{\partial T}{\partial z}\right)_{i+(1/2)}(z_{\mathrm{TP}} - z_i), & \text{if } z_{\mathrm{TP}} < z_i. \end{cases} \tag{A3}$$

Alternatively, the tropopause temperature has been computed by interpolation. Since the extrapolated temperature turned out to be significantly closer to the radio-

sonde-derived values (see Fig. 2d), it is used for the data analysis presented this study. Finally, the thickness criterion according to WMO (1957) is checked:

$$\text{for all } i \text{ with } 0 < z_i - z_{\text{TP}} \leq 2 \text{ km}:$$

$$\frac{T_i - T_{\text{TP}}}{z_i - z_{\text{TP}}} > -2 \text{ K km}^{-1}. \quad \text{(A4)}$$

If (A4) is not met, then the search for the tropopause is continued. As already mentioned in section 3a, the inclusion of (A4) is necessary. There are two possibilities that no tropopause is found until $p = 90$ hPa.

1) In all layers $(\partial T/\partial z) > -2$ K km$^{-1}$. In this case, which occurs extremely rarely in Arctic winter, the tropopause is set to 3.5 km above ground level (AGL).
2) In all layers, $(\partial T/\partial z) < -2$ K km$^{-1}$, or (A4) is never met. This sometimes occurs in Antarctic winter under strong cyclonic influence (see sections 7, 8). The tropopause is set to 90 hPa in this case.

Since the failure frequency amounts to only about $5 \times 10^{-6}$, it can be stated that the statistics presented in this study are not influenced by the cases where no regular tropopause is found.

## APPENDIX B

### Determination of the Dynamical Tropopause from the ERA Data

The algorithm used for the determination of the dynamical tropopause is similar to that described above except that the vertical temperature gradient is replaced by potential vorticity. The hydrostatic form of PV, written in $z$ coordinates, is used assuming that the ERA model levels are quasi-horizontal in the tropopause region:

$$P = \frac{1}{\rho}(f\mathbf{k} + \boldsymbol{\nabla} \times \mathbf{v}) \cdot \boldsymbol{\nabla}\theta. \quad \text{(B1)}$$

Here, $\rho$ is the density, $\mathbf{k}$ is the unit vector in the vertical and $\mathbf{v} = (u, v)$ is the horizontal wind vector. As above, (B1) is discretized on intermediate levels defined by $z_{i+1/2} := (z_i + z_{i+1})/2$ using centered differences:

$$P_{i+(1/2)} = \frac{R(T_i + T_{i+1})}{2\sqrt{p_i p_{i+1}}}(SX_{i+(1/2)} + SY_{i+(1/2)} + SZ_{i+(1/2)}), \quad \text{(B2)}$$

where

$$SX_{i+(1/2)} = -\left(\frac{\partial v}{\partial z}\right)_{i+(1/2)}\left(\frac{\Delta\theta}{\Delta x}\right)_{i+(1/2)};$$

$$SY_{i+(1/2)} = \left(\frac{\partial u}{\partial z}\right)_{i+(1/2)}\left(\frac{\Delta\theta}{\Delta y}\right)_{i+(1/2)};$$

$$SZ_{i+(1/2)} = \left(f + \frac{\zeta_i + \zeta_{i+1}}{2}\right)\left(\frac{\partial\theta}{\partial z}\right)_{i+(1/2)}$$

and $\Delta$ denotes centered horizontal differences. Since the relative vorticity $\zeta$ is one of the prognostic variables in a spectral model, no differencing is required to obtain $\zeta$. Then, the level that meets $P_{i-1/2} < P_{\text{TP}} \leq P_{i+1/2}$ is determined, $P_{\text{TP}}$ being the threshold value used as tropopause definition. Following Hoerling et al. (1991) and H98, $P_{\text{TP}} = 3.5$ PVU is used in the current study. As is discussed in section 3, the WMO threshold value of 1.6 PVU has been found to be inappropriate for higher latitudes. The tropopause height is set to

$$z_{\text{TP}} = z_{i-(1/2)} + (z_{i+(1/2)} - z_{i-(1/2)})\frac{P_{\text{TP}} - P_{i-(1/2)}}{P_{i+(1/2)} - P_{i-(1/2)}}, \quad \text{(B3)}$$

and tropopause pressure and temperature are calculated according to (A2) and (A3).

A thickness criterion similar to the second part of the thermal WMO criterion has been introduced into the PV-tropopause algorithm. It requires that the mean PV between the tropopause and all levels within 2 km above is greater than $P_{\text{TP}}$. Since the vertical distance of the ECMWF model levels varies little from one level to the next, this ''mean PV'' is simply computed by taking the arithmetic mean of the respective $P_{i+1/2}$ values calculated above. Omitting this thickness criterion induces no significant differences except in Antarctic winter over the Ross Ice shelf, where advection of stable air from the Antarctic continent sometimes induces a strong inversion near 550 hPa,[3] which may be misinterpreted as tropopause without the thickness criterion. It is noted that a thickness criterion like this is much more important when the dynamical tropopause is to be calculated from radiosonde data because thin layers of enhanced stability (e.g., subsidence inversions) are otherwise misinterpreted as tropopause (see appendix C).

Finally, an empirical correction of a systematical error is applied to this algorithm. From a simple geometrical consideration, it can be expected that the formula used for the calculation of the exact value of the tropopause height [Eq. (B3)] yields too large (too low) tropopause heights if the mean value of the PV below and above the tropopause is lower (higher) than the threshold value of the tropopause criterion (3.5 PVU). An analysis of the ERA-derived tropopauses revealed that such a correlation is indeed present. However, the calculation of the mean PV from the ERA data proved to be quite difficult. The problem is that there is usually one transitional model layer in the tropopause region that is neither representative for the upper troposphere nor for the lower stratosphere. Therefore, at least two model layers on each side of the tropopause should be taken into consideration. Assuming that the tropopause lies within $z_{i-1/2}$ and $z_{i+1/2}$ [see (B3)], min $(P_{i-1/2}, P_{i-3/2})$ may be taken as upper-tropospheric value, and max $(P_{i+1/2},$

[3] Near the Ross Ice Shelf, the Antarctic continent has a height of more than 4000 m (even in the model orography) and very steep slopes toward the coast. Therefore, offshore advection of the surface inversion layer causes an elevated inversion at about 550 hPa.

$P_{i+3/2}$) as lower-stratospheric value. Denoting the difference between the mean of these two values and $P_{\mathrm{TP}}$ as $\delta P$, the correction term

$$\Delta z_{\mathrm{TP}} := 0.24(z_{i+1} - z_i)(\delta P + 0.4\mathrm{PVU});$$

$$|\Delta z_{\mathrm{TP}}| \leq \frac{1}{2}(z_{i+1} - z_i) \tag{B4}$$

has been found to remove most of the systematical differences between ERA-derived and radiosonde-derived PV tropopauses. The superiority of PV tropopauses over thermal tropopauses revealed in Fig. 2a is partly due to this empirical correction. For the thermal tropopauses, we were not able to find a similar correction.

## APPENDIX C

### Determination of the Dynamical Tropopause from Radiosonde Data

The common way to compute the dynamical tropopause from radiosonde data is to perform an isentropic analysis (e.g., Bleck and Mattocks 1984). However, the density of radiosonde stations is too low in polar regions for this method to be used (see Fig. 1). Therefore, the vertical component of the vorticity $\zeta$ is interpolated from the ERA data. Since NWP analysis uses a lot of additional data sources (primarily from remote sensing) and produces dynamically consistent fields, the ERA vorticity is certainly more reliable than that computed from the radiosonde data alone. The interpolation is done for all radiosonde stations and all model levels. Then, the data are interpolated linearly in ln $p$ to the pressure levels where radiosonde data are available, that is, both standard and significant levels. For each level, two approximated PV values are computed, once using the temperature gradient below and once that above:

$$P_i^- = p_0^\kappa R T_i (f + \zeta_i)\left[\left(\frac{\partial T}{\partial z}\right)_{i-(1/2)} + \frac{g}{c_p}\right] p_i^{-(1+\kappa)}$$

$$P_i^+ = p_0^\kappa R T_i (f + \zeta_i)\left[\left(\frac{\partial T}{\partial z}\right)_{i+(1/2)} + \frac{g}{c_p}\right] p_i^{-(1+\kappa)}. \tag{C1}$$

Equation (C1) is obtained from the approximated PV formula $P \approx 1/\rho(f + \zeta)\partial\theta/\partial z$ by substituting $\partial\theta/\partial z = (\partial T/\partial z + g/c_p)(p_0/p)^\kappa$, where $p_0 = 1000$ hPa. If $P_i^- < P_{\mathrm{TP}}$ and $P_i^+ \geq P_{\mathrm{TP}}$ are met at some point $i$ of the sounding, then $p_i$ is taken to be the dynamical tropopause, provided that the thickness criterion (see below) is fulfilled. The other possibility is $P_i^+ < P_{\mathrm{TP}}$ and $P_{i+1}^- \geq P_{\mathrm{TP}}$. In this case, $p_{\mathrm{TP}}$ is interpolated between $p_i$ and $p_{i+1}$ under the assumption $P \sim \ln p$, and again, the thickness criterion is checked. In order to exclude the surface inversion, the search starts at $z = 3000$ m. If the station height is above 1500 m, the starting point is set to 1500 m above ground. Only the lowest tropopause is taken for the analysis presented here.

The thickness criterion requires, as for the ERA tropopause, that the mean PV between the tropopause and all higher data points within 2 km is greater than $P_{\mathrm{TP}}$. Since a sounding has irregularly spaced data points, the mean PV is calculated according to

$$(\overline{P_{\mathrm{TP}}})_i = p_0^\kappa R \frac{T_{\mathrm{TP}} + T_i}{2}\left(f + \frac{\zeta_{\mathrm{TP}} + \zeta_i}{2}\right)\left(\frac{T_i - T_{\mathrm{TP}}}{z_i - z_{\mathrm{TP}}} + \frac{g}{c_p}\right) \times (\sqrt{p_{\mathrm{TP}} p_i})^{-(1+\kappa)}. \tag{C2}$$

A sensitivity study has been made by using different thickness criteria. For thickness values below 1000 m, results have been found to be highly sensitive to changes of the thickness. In particular, the correlation coefficient between ERA-derived and radiosonde-derived tropopauses (see Fig. 2c) decreases dramatically for low thickness values. If, for example, a value of 300 m is used, the correlation coefficients range between 0.4 and 0.8 compared to 0.9–0.95 for a value of 2 km (Fig. 2c). For values of 1500 m or more, there is virtually no sensitivity. Therefore, a thickness criterion using a value of 2000 m can be regarded as meaningful. Finally, it is noted that the dynamical tropopauses computed from the radiosondes are not very sensitive to the exact value of the relative vorticity. In most cases, the dynamical tropopauses coincide with a significant level, that is, a change in vertical temperature gradient, so that small changes in the relative vorticity would have no influence on the results.

## REFERENCES


Appenzeller, Ch., J. R. Holton, and K. H. Rosenlof, 1996: Seasonal variation of mass transport across the tropopause. *J. Geophys. Res.*, **101,** 15 071–15 078.

Bethan, S., G. Vaughan, and S. J. Reid, 1996: A comparison of ozone and thermal tropopause heights and the impact of tropopause definition on quantifying the ozone content of the troposphere. *Quart. J. Roy. Meteor. Soc.*, **122,** 929–944.

Court, A., 1942: Tropopause disappearance during the Antarctic winter. *Bull. Amer. Meteor. Soc.*, **23,** 220–238.

Ebel, A., H. Elbern, J. Hendricks, and R. Meyer, 1996: Stratosphere–troposphere exchange and its impact on the structure of the lower stratosphere. *J. Geomagn. Geoelectr.*, **48,** 135–144.

Frederick, J. E., and A. R. Douglass, 1983: Atmospheric temperatures near the tropical tropopause: Temporal variations, zonal asymmetry and implications for stratospheric water vapor. *Mon. Wea. Rev.*, **111,** 1397–1403.

Grewe, V., and M. Dameris, 1996: Calculating the global mass exchange between stratosphere and troposphere. *Ann. Geophys.*, **14,** 431–442.

Highwood, E., and B. J. Hoskins, 1998: The tropical tropopause. *Quart. J. Roy. Meteor. Soc.*, **124,** 1579–1604.

——, ——, and P. Berrisford, 2000: Properties of the Arctic tropopause. *Quart. J. Roy. Meteor. Soc.*, **126,** 1515–1532.

Hoerling, M. P., T. K. Schaack, and A. J. Lenzen, 1991: Global objective tropopause analysis. *Mon. Wea. Rev.*, **119,** 1816–1831.

Hoinka, K. P., 1998: Statistics of the global tropopause pressure. *Mon. Wea. Rev.*, **126,** 3303–3325.

——, 1999: Temperature, humidity and wind at the global tropopause. *Mon. Wea. Rev.*, **127,** 2248–2265.

Holton, J. R., 1990: On the global exchange of mass between the stratosphere and troposphere. *J. Atmos. Sci.*, **47,** 392–395.

——, P. H. Haynes, M. E. McIntyre, A. R. Douglass, R. B. Rood, and L. Pfister, 1995: Stratosphere–troposphere exchange. *Rev. Geophys.*, **33,** 403–439.

Hoskins, B. J., M. E. McIntyre, and A. W. Robertson, 1985: On the use and significance of isentropic potential vorticity maps. *Quart. J. Roy. Meteor. Soc.*, **111,** 877–946.

Möller, F., 1938: Der Jahresgang der Temperatur in der Stratosphäre. *Meteor. Z.*, **55,** 161–170.

Naujokat, B., 1992: Stratosphärenerwärmungen: Synoptik. Meteorologie der Mittleren Atmosphäre. *Promet*, **22** (2–4), 81–89. [Available from Deutscher Wetterdienst, D-63004 Offenbach, Germany.]

——, and K. Labitzke, Eds.,1993: Solar-Terrestrial Energy Program: Collection of reports on the stratospheric circulation during the winters 1974/75–1991/92. Stratospheric Research Group, Free University Berlin, 306 pp. [Available from SCOSTEP Secretariat, University of Illinois at Urbana, 1406 W. Green Street, Urbana, IL 61801.

Newell, R. E., and S. Gould-Stewart, 1981: A stratospheric fountain? *J. Atmos. Sci.*, **38,** 2789–2796.

Reed, R. J., 1955: A study of a characteristic type of upper-level frontogenesis. *J. Meteor.*, **12,** 226–237.

Reid, G. C., and K. S. Gage, 1996: The tropical tropopause over the western Pacific: Wave driving, convection, and the annual cycle. *J. Geophys. Res.*, **101,** 21 233–21 241.

Rosenfield, J. E., M. R. Schoeberl, and M. A. Geller, 1987: A computation of the stratospheric diabatic circulation using an accurate radiative transfer model. *J. Atmos. Sci.*, **44,** 859–876.

Shapiro, M. A., 1980: Turbulent mixing within tropopause folds as a mechanism for the exchange of chemical constituents between the stratosphere and troposphere. *J. Atmos. Sci.*, **37,** 994–1004.

van Haver, P., D. De Muer, M. Beekmann, and C. Mancier, 1996: Climatology of tropopause folds at midlatitudes. *Geophys. Res. Lett.*, **23,** 1033–1036.

Wirth, V., 1995: Diabatic heating in an axisymmetric cut-off cyclone and related stratosphere–troposphere exchange. *Quart. J. Roy. Meteor. Soc.*, **121,** 127–147.

——, 2000: Thermal versus dynamical tropopause in upper tropospheric balanced flow anomalies. *Quart. J. Roy. Meteor. Soc.*, **126,** 299–317.

WMO, 1957: Meteorology—A three dimensional science. *WMO Bull.*, **6,** 134–138.

——, 1986: Atmospheric ozone 1985. Global ozone research and monitoring report. WMO Rep. 16, 392 pp.

Yulaeva, E., J. R. Holton, and J. M. Wallace, 1994: On the cause of the annual cycle in tropical lower-stratospheric temperatures. *J. Atmos. Sci.*, **51,** 169–174.